University of Washington
Department of Bioengineering
Capstone Project Thesis

ANTI–CANCER NANOPODS:

RATIONAL DESIGN OF AN OLIGOARGININE BASED GENE DELIVERY VEHICLE TARGETED TO HEPATOCARCINOMA

Kathy Y. Wei
Student ID: 0521502
Email: kwei@u.washington.edu
Date: Friday June 9, 2009

Faculty Mentor: Dr. Suzie Pun

ABSTRACT

Each year, liver cancer is diagnosed in 20,000 new patients in the United States and causes 662,000 deaths worldwide, making it one of the three deadliest cancers in the world. Current treatments, such as surgery, transplant, and chemotherapy, involve significant damage to healthy tissue and can typically only extend the life of patients for about a year after diagnosis. Gene therapy, which aims to replace defective genes inside cells in order to treat diseases, holds promise for treating liver cancer because of the various pathways it can exploit. For instance, one could alter a patient's immune system to recognize cancerous cells, replace the malfunctioning genes needed for proper cell regulation and function, or enhance the sensitivity of cancer cells to chemotherapy. Modified viruses have been used for gene therapy, but their use is limited by safety concerns and large-scale production difficulties. Non-viral materials have the potential to overcome these concerns, but they are currently limited by inefficient delivery and nonspecific binding. The goal of this project is to design, construct, and test novel peptide-based materials specifically targeted to hepatocarcinoma, which is the most common form of primary liver cancer, for use as systemically administered gene therapy vectors. The peptide material consists of a nonaarginine DNA condensing component linked to a hepatocarcinoma-specific binding peptide (sequence: FQHPSFI). This material will form an anti-cancer "nanopod" that both protects the DNA therapeutic from degradation and acts as a guidance system to deliver the genes preferentially to the target. Successful completion of this project will result in an efficient, specific gene therapy delivery vehicle that can be further developed into an effective treatment for liver cancer.

TABLE OF CONTENTS

LIST OF FIGURES

CHAPTER 1: INTRODUCTION

1.1 Project Definition

This project attempts to address the inefficiency and non-specificity considerations of current non-viral gene delivery systems by developing a safe and customizable vehicle to be systemically delivered and specifically targeted to liver cancer. Materials will be designed by rationally combining various small functional peptide and carbohydrate components identified from literature. As illustrated in Figure 1.1, the specific components of this modular vehicle will be: 1) a model plasmid DNA therapeutic (gWiz Luciferase), 2) a DNA condensing component to form nanoparticles with and condense the DNA therapeutic and may also have cell-penetrating functionality (nona-L-arginine (R9)), 3) a cell targeting compound to specifically deliver the vehicle to hepatocarcinoma cells (seq: FQHPSFI (TP) and galactose (Gal)), and 4) a linker to chemically conjugate the DNA condensing and cell targeting components as well as provide flexibility to allow components to function with minimal steric hindrance (DSS). These peptide-based materials will act as an anti-cancer "nanopod" that provides protection for the DNA therapeutic and acts a guidance system to deposit the genes preferentially to the target cells. The general concepts in this peptide design can be extended to create novel gene therapy treatments that target any cell-type-specific disorders, including other cancers.

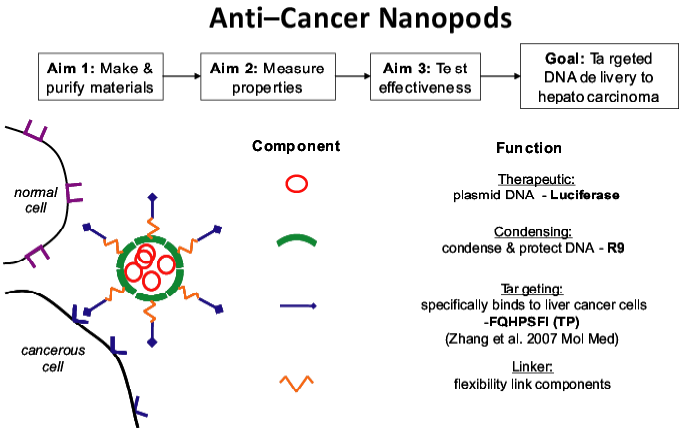

Figure 1.1: Overview of the anti-cancer nanopod project.

Specific Aim 1: Synthesis and Purification

Construct, and purify materials to be used in non-viral gene delivery to liver cancer (hepatocarcinoma) cells.

- Design protocol(s) for synthesis such that: 1) product is pure, 2) product yield is high, and 3) protocol uses available materials and equipment.
- Design protocol(s) for purification based on the natures of the peptide and contamination (ex. size, charge, hydrophobicity).

Specific Aim 2: Characterization

Characterize the physical and chemical properties of the various nanopods (peptide material + plasmid DNA) using established techniques.

- Characterize DNA complexation ability of the peptides by YOYO1 quenching assay.
- Characterize size and surface charge of the nanopods by dynamic light scattering.
- Characterize cell toxicity of the nanopods by MTS assay.

Specific Aim 3: Evaulation

Evaluate for statistically significant increase of targeted nanopods at delivering DNA (transfection) and binding to hepatocarcinoma cells.

- Evaluate transfection efficiency by luciferase assay.
- Evaluate cell binding by flow cytometry.

1.2 Significance

1.2.1 Liver Cancer and Current Limitations to Treatment

The World Health Organization estimates that each year, liver cancer causes 662,000 deaths world-wide, making it one of the three deadliest cancers. According to the National Cancer Institute, there are approximately 20,000 new cases each year in the United States alone. The prognosis for liver cancer is almost never good. If caught early, surgery is an effective option, but because liver cancer is usually asymptomatic until late into its progression, this is rarely the case (Collier). Patients typically live from 3 months to 18 months after diagnosis, even with treatment.

All currently available treatments have undesirable limitations. Surgery is restricted to patients with small tumors before metastasis. Although tumors are removed, the inherent problem is not necessarily eliminated and relapse is highly possible (Gérolami 2003). Liver transplants are currently the best approach if the tumor is inoperable, but finding appropriate matches is difficult and does not preclude recurrence. Other common cancer treatments, such as radiation therapy and chemotherapy, are highly toxic procedures and are known to damage normal as well as diseased tissues. Such treatments rely on a fine balance between killing enough cancer cells before killing too many normal cells. These therapies are associated with harsh side effects such as bone marrow suppression, severe nausea, vomiting, and hair loss.

Patients often need further medication in an attempt to ameliorate the side effects of their treatment, compounding patient burden in terms of treatment complexity and cost. One of the major symptoms of liver cancer is a high degree of pain and thus necessitates the use of even

more drugs in order to make the patient as comfortable as possible. Clearly, there is a need to develop better treatment options.

1.2.2 Gene Therapy for Liver Cancer

Gene therapy, or the alteration of genetic information of cells to treat diseases, is promising for treating liver cancer because of the multiple treatment pathways that can be exploited. Gene therapy can potentially alter a patient's immune system to recognize cancerous cells, replace the malfunctioning genes needed for proper cell regulation and function, enhance the sensitivity of cancer cells to chemotherapy, confer resistance to chemotherapeutics to normal cells to limit side effects of chemotherapy, and much more. Some of these capabilities, like altering a patient's immune system, may be capable of conferring long-term cancer suppression and become a cure.

However, one of the major challenges to gene therapy is the development of safe and effective ways deliver genes to specific targets. Modified viruses have traditionally been used as vectors in gene delivery because they have evolved sophisticated mechanisms for introducing genetic material into mammalian cells. Some viruses commonly used include retrovirus, lentivirus, adenovirus, adeno-associated virus (AAV), herpes simplex virus, and pox virus. Gene therapy was first demonstrated in clinical trials to be effective for treating severe combined immune deficiency (SCID) using viruses (Cavazzana-Calvo 2000). However, three years later, two of the patients treated developed cancers (Hacein-Bey-Abina 2003). The deaths of Jesse Gelsinger in 1999 and Jolee Mohr in 2007 during clinical trials involving gene therapy have shaken the public confidence in the field (Hughes).

There are several safety issues that arise from the use of viruses. Although the viral genetic material is removed, there is a possibility that modified viruses can regain their self-replicating ability by mutation or by coming into contact with viruses that can replicate. Viruses can also mediate random integration of the delivered gene into chromosomes, which could result in undesirable outcomes. Researchers have also shown that in mice, injection of AAV was correlated with the development of liver tumors (Donsante 2007). Although there is controversy over whether the correlation extends to humans, the concern remains. Some viral particles also elicit an immune response. This can cause a severe reaction in the patient and restricts the application of the treatment to a single dose because the patient will quickly clear the vector after the first exposure.

The potential dangers of viral vectors motivate the development of non-viral gene delivery materials, which are potentially safer and more controllable than modified viruses. Non-viral gene delivery materials currently being studied range from non-organic substances such as gold and iron oxide to organic substances like lipids and polymers. Plasmid DNA and cationic lipids or polymers that self-assemble into nanoparticles due to electrostatic interactions are generally known as lipoplexes and polyplexes, respectively (Pack 2005). The major challenge is that these non-viral materials are currently orders of magnitude less efficient than viruses. The goal of this project to design a novel non-viral material that overcomes the inefficiency of current materials and specifically targets hepatocarcinoma, the most prevalent form of primary liver cancer (Gérolami 2003).

1.3 Broader Impact

1.3.1 Social and Ethical Considerations

The first successful clinical gene therapy trial treated infants with severe combined immune deficiency (SCID) in 2000 (Cavazzana-Calvo 2000). However, three years later, two patients developed cancers (Hacein-Bey-Abina 2003). In this trial and in most gene therapy clinical trials, viruses are used to deliver DNA. While the viral genetic material is removed, there are concerns that modified viruses can regain their self-replicating ability by mutation or insert therapeutic DNA randomly into chromosomes. Viruses can also cause severe allergic reactions. As reported in Nature News, several cases of fatalities during gene therapy trials have occurred, including Mohr during arthritis treatment and Gelsinger during ornithine transcarbamylase deficiency treatment (Hughes).

As reported in Nature News, although more than 1,300 gene therapy trials worldwide have been conducted, as of 2007, only one has been marketable. Considering the risks of gene therapy and the lack of large scale success for any particular treatment, gene therapy may not seem to be a viable option. However, risk is associated with the development of any new drug or therapy. The trials and facts presented above are biased because the benefits do not necessarily outweigh the risks in these cases. This important principle from the Belmont Report is satisfied if, as in the case of this project, the target disease for the therapy is fatal and for which there is no satisfyingly effective available treatment. The risks associated with using viruses

are also the motivation to design better non-viral gene delivery systems, which potentially avoid the safety issues involved with viruses.

The development of truly effective gene therapies is also controversial because the techniques could potentially be used to enhance physical or even mental characteristics in people. Unequal access to gene therapy enhancement will provide certain individuals an unfair advantage in such activities as athletic competitions or employment. Although the United States government voted in 2008 to disallow genetic discrimination, there is no regulation on favoring better health, or greater skills and talents. The increase in the disparity between those who can and cannot afford gene enhancement can quickly become a major source of concern worldwide. However, this can be avoided by government regulation at all levels to ensure equitable distribution of resources.

1.3.2 Regulatory Considerations

The anti-cancer peptide based gene delivery nanopods produced by this project will be a proof-of-concept product to demonstrate the possibility of designing a safe and effective systemically delivered gene therapy treatment for liver cancer. Extensive *in vivo* studies in mice and larger mammals are needed to determine toxicity levels and effective dosages. Clinical trials will of course be necessary to determine that the newly developed materials do not result in unacceptable side effects, and to refine dosage regiments in humans. The materials must obtain FDA approval and institutions associated with human subjects must comply with human subject regulations and if any gene insertions are involved, advance approval by the Institutional Biosafety Committee is needed. Each human gene therapy proposal must also be approved by the Director of the NIH (NIH).

1.3.3 Commercialization and Marketing Considerations

Once the safety and effectiveness of the material is established and a proper therapeutic plasmid is developed to be combined with the R9 and TP conjugation, the overall therapeutic product may have potential to be patented. The non-viral material to be developed is a small peptide and can be made by in large amounts by prokaryotic cell systems or by chemical synthesis. Since the product is designed for systemic delivery, no equipment beyond currently available syringes and needles will be necessary. Treatment protocol will be similar to

immunization shots and will require minimal training. Doctors will need to be trained to properly gauge the dosage and frequency of the treatment needed on a patient to patient basis, similar to current chemotherapy.

A large market for this new cancer treatment is China, which has more than 50% of worldwide liver cancer cases (pharmalicensing.com). The market can then expand into the US and European market (worth some $850 mill). Treatment is expected to give revenues of $165 mill a year for the first five years, if comparable to Nexavar from Onyx pharmaceuticals. Treatment costs will have to be carefully optimized because cost is a major limiting factor in the Chinese market.

1.4 Technical Background

1.4.1 Barriers to Gene Delivery

Non-viral gene delivery methods offer a potentially safer, more flexible, and more controllable alternative to viral gene delivery systems. The range of non-viral compounds currently under investigation is vast, including cationic lipids (Felgner 1987), polymers (Boussif 1995), dendrimers, cyclodextrin (Gonzalez 1999), and peptides. The current limitation of non-viral materials is their relative inefficiency at transfecting, or transferring exogenous genetic information, to mammalian cells. This is hypothesized to be due to the lack of ability to overcome both the extracelluar and intracellular barriers to delivery (Pack 2005, Martin 2007). Viral vectors are more effective because they have evolved sophisticated mechanisms to overcome these challenges. The barriers include 1) DNA packaging, 2) cell targeting, 3) cell internalization, 4) endosomal escape, 5) nuclear localization, and 6) nuclear internalization. The specific barriers will change depending on the route of administration, target cell type, and nature of the disorder, among other factors. For example, oral delivery systems must also consider the pH conditions encountered in the digestive system and the amount of therapeutic absorbed. In terms of cell types, delivery to non-dividing cells such as neurons is especially challenging because the intact nuclear membrane.

This investigation addresses DNA packaging, cell-specific targeting, and cell internalization. DNA condensation is generally necessary to protect DNA from degradation by DNase by sterically blocking access to the DNA. Naked DNA is degraded within minutes while DNA complexed with polymers remains stable for hours (Abdelhady 2003). When nucleic acids are condensed into particles of less than a few

hundred nanometers in diameter through electrostatic interaction with a polymer to form polyplexes, generally at least six to eight cationic moieties are required (Plank 1999, Schaffer 2000, Wadhwa 1997). Stronger condensation however, does not directly correlate to more efficient transfection because it is hypothesized that complexation can prevent transcription. Therefore, a balance between initial nucleic acid packaging and eventual un-packaging is necessary for optimal gene expression (Pack 2005)

Cell targeting is an example of an application dependent barrier. In the case of cancer treatment, highly specific targeting is desired to mitigate damage to off-target tissue, which is the source of the highly undesirable side-effects of current chemotherapeutics. The classic and still commonly used hepatocyte cell surface target has been the asialoglycoprotein (ASGP) receptor and the classic targeting moiety has been galactose (Sagara 2002, Zanta 1997). Many other targeting moieties, ranging from small molecules such as thyroid hormone (Rudolph 2007), to proteins like lactoferrin (Weeke 2007) have been used to improve gene delivery to hepatocytes. The success of targeting depends strongly on the specific conjugation chemistry, linker length, ligand-receptor strength, and the number of targeting ligands per polymer (Pack 2005, Sagara 2002). Because the cell surface is overall negatively charged, positive particles will nonspecifically bind to cells. Thus, the specificity of targeting interactions requires a polymer/DNA ratio that forms a near neutral polyplex to balance between the specific and non-specific forces (Schaffer 1998).

Cellular uptake of polyplexes is mediated by nonspecific adsorptive pinocytosis or by specific receptor-mediated endocytosis (Pack 2005). In the case of small molecule drugs, the compound must be polar enough to be soluble in the body to allow proper distribution, yet nonpolar enough tot diffuse across cell membranes (Wender 2000). Ways to modify the solubility include chemical modification, formulation conditions, or encapsulation in liposomes (Wender 2000). The efficiency of internalization can also be increased by utilizing moieties that provide active transport across cell membranes. A classic example is HIV-1 derived sequence peptide Tat (Kosuge 2008). Although the mechanism of transport is unknown, the Tat peptide has been used to deliver a number of different biomolecules into cells, including an inhibitor of HPV (Pepinsky 1994), ovalbumin into MHC class I pathyway (Kim 1997), Cdk inhibitors $p27^{Kip1}$ (Nagahara 1998), and $p16^{INK4a}$ (Gius 1999), caspase-3 protein (Vocero-Akbani 1999), and β-galactosidase i*n vivo* into all tissues of mouse (Schwarze 1999). Other examples of cell-penetrating peptides include sequences derived from Antennapedia (Derossi 1998, Lindgren 2000), fibroblast

growth factor (Lin 1995), transportan (Pooga 1997), HSV-1 protein VP22 (Elliott 1997), and oligoarginine (Kosuge 2008, Wender 2000)

1.4.2 Peptide Based Gene Delivery

Peptides offer an advantage over other non-viral agents because they are able to address the barriers to gene delivery as well as the technical considerations for manufacturing. The vast natural diversity of proteins indicates that peptide-based vehicles have the functional diversity to overcome all of the barriers to gene delivery (Martin 2007). Natural systems also indicate that peptides can be highly modular. Small sections of proteins can be sufficient to afford a desired function, such at the Tat sequence derived from HIV-1 (Vives 1997) or influenza HA-2 N-terminal peptides (Wagner 1992) for cell membrane penetration. By reverse engineering this process, peptides with different function can be combined to carry out complex tasks.

In terms of manufacturing, small peptides are simple and relatively inexpensive to fabricate and purify. They also tend to be safer in terms of toxicity, immunogenicity, and pathogenicity. In contrast, for standard polycationic polmers such as PLL and PEI, transfection activity is correlated with membrane toxicity. Larger, more cytotoxic polymers are more effective (Thomas 2003).

1.4.3 Oligoarginines

Nona-L-arginine (R9) is used in this project mainly as a DNA condensing material, but oligoarginines are also cell-penetrating peptides and may also impart increased cellular uptake in the system studied. There is precedent that a single peptide can be involved in multiple functions. Specifically, the nuclear localization sequence of SV40 large T antigen is involved in both nuclear targeting as well as electrostatically condensing DNA in a peptide-based gene delivery system for siRNA (Simeoni 2003).

Cell penetrating peptides are often used to enhance the delivery of various cargo, including small molecules, peptides, proteins, oligonucleotides, and liposomes (Kosuge 2008, Snyder 2005, Wender 2000). Although the HIV-1 derived Tat peptide is a classic example of a cell-penetrating peptide, nona-L-arginine has been shown to be 20-fold more efficient than Tat_{49-57} at cellular uptake (Wender 2000). The specific mechanism of internalization is unknown, but guanidinium groups appear to contribute more to cellular internalization than either the charge or backbone structure of a cell-penetrating peptide

(Wender 2000). There is also evidence that oligoarginines are can distribute to the endosome or diffusely to the cytoplasm, depending on the peptide concentration, temperature of incubation, and presence of serum (Kosuge 2008).

Oligoarginines have successfully been incorporated into vectors for improved delivery. For example octaarginine-modified nanoparticles achieved transfection similar to adenovirus-mediated transfection while maintaining lower cytotoxicity (Khalil 2007), oligoarginine enhanced uptake of tumor antigens over PLL by 10-fold (Buschle 1997), and nonaarginine conjugations to targeting peptides have been successfully used to bind siRNA and achieve gene silencing *in vitro* and *in vivo* (Kumar 2007).

1.4.4 Targeting Peptides

A general problem with currently available drugs, and especially chemotherapeutics, is the lack of precise selectivity (Sachdeva 1998, Torchilin 2000). Peptides are especially useful for targeting in cancer treatment because they are small and thus afford better tumor penetration and less immunogenicity (Otte 1998).

Targeting peptides can be identified from studying natural systems, like the nontoxic fragment C of tetanus toxin to target nerve cells (Knight 1999) and 19-amino peptide derived from circumsporozoite protein of *Plasmodium berghei* to target liposomes to hepatocytes (Longmuir 2006). An alternative method is to use phage display to screen peptide libraries for high cell or tissue specificity (Nilsson 2000, Smith 1985, Zurita 2003). Phage display has been specifically applied to identifying peptide sequences specifically targeted to hepatocarcinoma such as 12-mer TACHQHVRMVRP (Du 2006) with selectivity of approximately 2.2 over control cells and 7-mer FQHPSFI (Zhang 2007) with selectivity of 2.5 over control cells.

Interesting, the 7-mer sequence FQHPSFI identified by phage display used investigated here matches a hypothetical protein in *Entamoeba histolytica* according to a NIHG protein BLAST of the sequence. This is a pathogenic protozoan that usually invades the liver (Sherris Medical Microbiology).

1.5 Previous Relevant Pun Lab Work

The Pun lab has previously done work in liver as well as used functional peptides to improve the efficiency of non-viral gene delivery. The group has previously shown that exposing polyplexes to unpackaging conditions (such as serum or proteoglycans) *in vitro* will decrease

cellular uptake and that extensive unpackaging occur *in vivo* when polyplexes are injected intravaneously to the liver (Burke 2008). Thus, the anti-cancer nanopods in this project were designed to incorporate a DNA condensing component to protect that DNA as well as mediate uptake.

In general, the Pun lab has been able to show that peptides capable of overcoming various barriers to gene delivery can be successfully incorporated into non-viral gene delivery vehicles to improve delivery of DNA as well as siRNA. Typically, peptides have been conjugated to cationic polymers, such as PEI or PLL because this has been empirically determined to be more effective then simply adding the peptide in solution.

One example of a functional peptide studied in the lab is the membrane-lytic HIV gp41 endodomain derived peptide (HGP). This peptide was shown to increase transfection in and siRNA knockdown in HeLa cells when conjugated to PEI, hypothetically by increasing endosomal escape of the polyplexes (Kwon 2008 Bioconj Chem.). Much of the peptide based work was previously been done in neurons, specifically on Tet1, a peptide identified by phage display to target neurons. This peptide functions like the heavy chain protein of tetanus toxin and uses the same receptor (Park 2007). The lab has previously shown that when conjugated to PEI, the resulting Tet1-PEI nanoparticles showed 16.3% ($p< 0.001$) higher percent cellular binding to PC-12, neuron-like cells, than PEI as well as higher transfection than PEI (Park 2007). This demonstrates that targeting peptides can significantly improve delivery.

One of the goals of the lab is to develop a system for combining functionalities in a modular manner. In theory, multifunctional vehicles that can overcome multiple barriers would afford even higher efficiency than vehicles with only endosomal escape or only targeting. In previous work, both HGP and Tet1 were conjugated to PEI. These Tet1-PEI-HGP constructs where shown to increase expression by 9-fold compared to PEI-HGP ($p < 0.01$) and 2-fold compared to Tet1-PEI ($p<0.05$) (Kwon 2008 J Controlled Rel). However, for siRNA delivery, although HGP increased knockdown of GAPDH compared to PEI, Tet1 did not as either PEI-Tet1 or Tet1-PEI-HGP (Kwon 2008 J Controlled Rel).

This project also utilizes functional peptides, but does not use PEI as a base material. One of the major problems with attaching peptides onto a polymer is the lack of control and consistency in the amount and distribution of peptide on the polymer. The all-peptide approached used in this project is essentially an extension of the peptide work done thus far in the lab, but investigates a different format for using and combining functional moieties for gene delivery.

CHAPTER 2: DESIGN OF EXPERIMENTS

2.1 Overview of Design and Revisions

The flow-chart below depicts the design and revision process of the project. Blue text indicates paths that were taken. Explanations are provided in section 2.2.

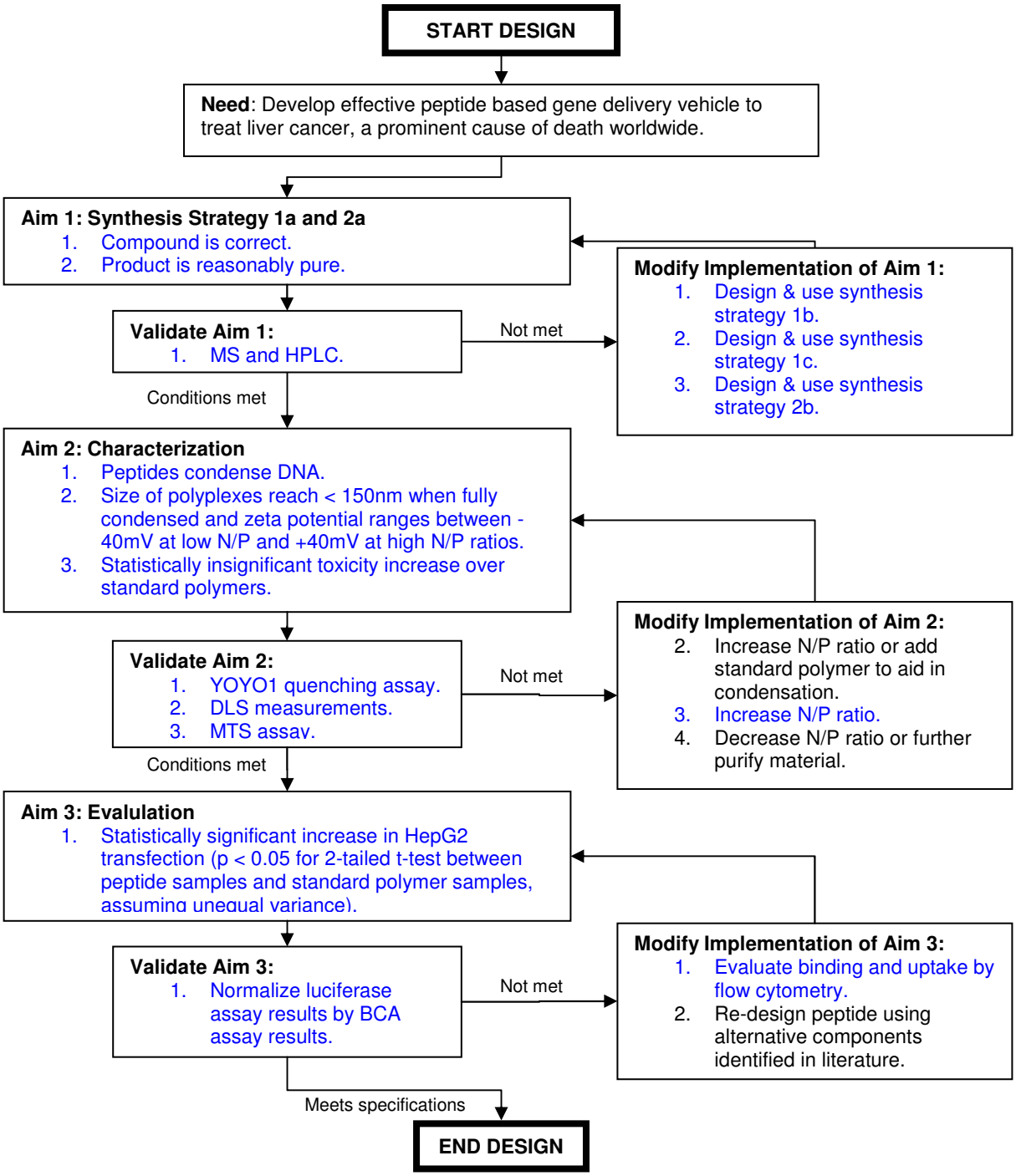

2.2 Explanation of Design and Revisions

2.2.1 Synthesis Strategy 1a: Solid Phase Peptide Synthesis (product: R9-G3-TP)

The peptides of interest are R9 (for electrostatically condensing DNA and potential to increase cellular uptake) and TP (for targeting). However, to prevent R9 and TP from sterically hindering the function of each other, three glycines were added as a flexible linker between the two. Of all the amino acids, glycine offers the most flexibility. At least a few glycines are needed to provide sufficient flexibility, but too many may cause the peptide to be excessively long and introduce aggregation issues. The original strategy was to use FMOC solid–phase-peptide-synthesis (SPPS) to synthesize the peptide sequence RRRRRRRRRGGGFQHPSFI.

2.2.2 Synthesis Strategy 1b: Heterobifunctional Crosslinking (product: R9-SS-TP)

Initial mass spectrometry and HPLC results indicated that the R9-G3-TP peptide was not synthesized successfully. The hypothesis was that the arginines were difficult to assemble, due to the chemical composition and the flexibility of the three glycines. Therefore, the peptide was deemed too challengin to synthesize with high fidelity and that a strategy which called for synthesis of the peptides in smaller pierces had higher chance of success. Also, since a crosslinking strategy would be necessary to attach galactose to R9 (as a control), developing a strategy that could be used to attach TP or galactose to R9 would be desirable because it reduces the number of differences between the two conjugates.

Heterobifunctional crosslinkers were chosen to avoid off target reactions (such as conjugation of R9 with R9). The amine ends of the R9 and TP peptides were modified such that they would be selectively reactive toward each other. Specifically, the heterobifunctional crosslinkers SMPB (reactive toward amino and sulfhydryl groups) and SATP (reactive toward amino and maleimide groups) were conjugated to TP and R9, respectively. The SATP-R9 was left on the resin so that excess hydroxylamine during the sulfhydryl deprotection step could be easily removed. Finally, SMBP-TP was conjugated to SATP-R9 to form R9-SS-TP. This synthesis scheme is presented in Figure 2.1.

2.2.2.1 Peptide Synthesis

Initially, peptides were made using HBTU as the amino acid Coupling Reagent, DMF as the Solvent, and piperidine as the Deprotector. However, because the resulting R9 peptides contained significant amounts of R8 and R7 contamination, the protocol was

modified to use HATU as the Coupling Reagent (for synthesis of R9), 50%DMF/50%DMSO as the Solvent, and 2%DBU/2% Piperidine as the Deprotector. These changes were shown empirically to increase purity of peptides synthesized by members of the laboratory.

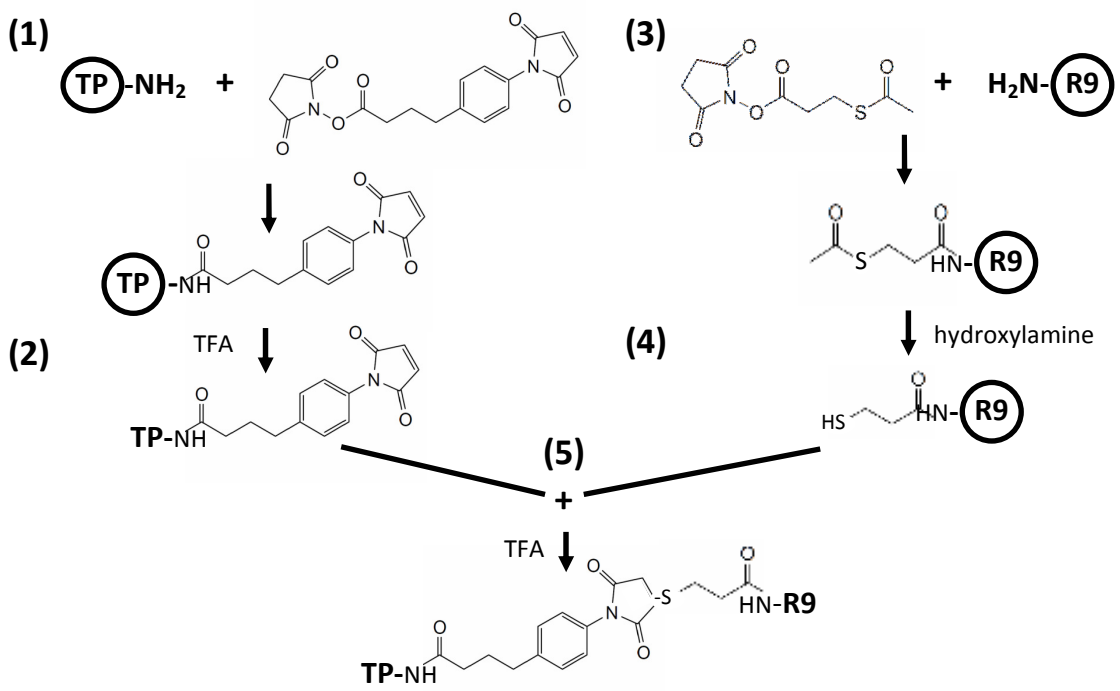

Figure 2.1: Schematic of synthesis strategy 1b: heterobifunctional crosslinking. Step 1 & 2: Attach SMPB to TP while peptide is still on the resin, and then cleave peptide off the resin using TFA. Step 3 & 4: Attach SATP to R9 while peptide is still on the resin and then deprotect the sulfhydryl on the SATP using hydroxylamine. Step 5: Conjugate peptides together and cleave the final product off the resin using TFA.

2.2.3 Synthesis Strategy 1c: Homobifunctional Crosslinking (product: R9-DSS-TP)

The last step of the heterobifunctional linking protocol could not be carried out adequately because the hydroxylamine was insoluble in organic solvent while the peptide resin was insoluble in aqueous solvent. In order to limit the number of steps, and therefore the complexity of the new reaction, a homobifunctional linker was chosen in the design of the new synthesis scheme, shown in Figure 2.2. Specifically, DSS was chosen for its ability to link the amine ends of the peptides together, high solubility in organic solvents, reasonable linker length, and compatibility with DIC/NHS chemistry (both of which are soluble in organic solvent).

Empirically, TP was soluble in DMF while R9 was not, so R9 was left on the resin. DIC/NHS chemistry is used to regenerate maleimide groups on DSS. Although DCC is the

more commonly used compound relative to DIC, it forms a precipitant that is difficult to purify away from the resin (Wipf). DIC has been used to attach linkers to functional groups on Wang resins the type of resin used in this case (Wipf). Also, DIC and DCC are equally effective (Hudson 1988), so it was the reagent of choice for this protocol.

No purification was done until all synthesis and conjugation reactions were complete to conserve material and time.

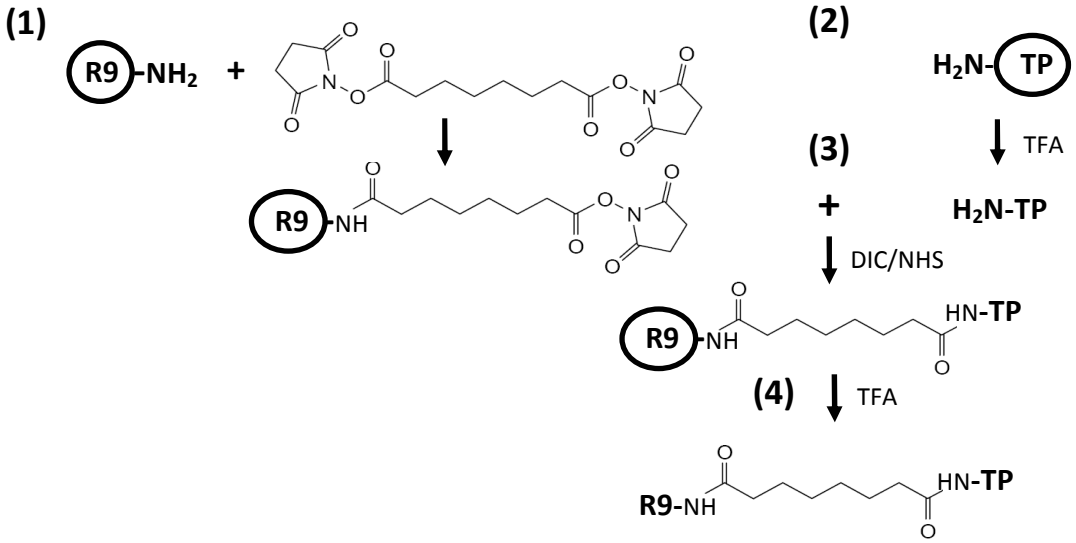

Figure 2.2: Schematic of synthesis strategy 1c: homobifunctional crosslinking. Step 1: Attach DSS to R9 while the peptide is still on the resin. Step 2: TP is cleaved from the resin using TFA. Step 3: TP in solution is added to R9-DSS, using DIC/NHS chemistry to regenerate maleimide groups on DSS. Step 4: The final produce, R9-DSS-TP, is cleaved from the resin using TFA.

2.2.4 Synthesis Strategy 2a: Synthesis with Galactosamine

Galactose is a commonly used targeting moiety for hepatocytes and serves as a control for the phage display identified targeting peptide, TP (Sagara 2002, Zanta 1997). Galactosamine, which has a free amine group analogous to that on TP, was to be attached to R9-DSS using same protocol for synthesizing R9-DSS-TP.

2.2.5 Synthesis Strategy 2b: Synthesis with Galactopyranoside (product: R9-DSS-Gal)

It was empirically determined that galactosamine was not soluble in DMF at the concentrations desired for the reaction, even after several hours incubation at 60^{o}C. Thus 4-aminophenyl β-D-galactopyranoside, which is soluble in DMF and previously used for targeting (Sagara 2002, Zhu 2008), was substituted for galactosamine.

2.3 Costs

	Full Name	Amount	Company	Cost
Peptide Synthesis				
R resin	Fmoc-Arg(Pbf)-Wang resin	1 g	Novabiochem	$81.00
I resin	Fmoc-Ile-Wang resin	1 g	Novabiochem	$22.00
Crosslinkers				
SMPB	Succinimidyl 4-[p-maleimidophenyl]butyrate	50 mg	Pierce	$89.45
SATP	*N*-Succinimidyl-S-acetylthiopropionate	50 mg	Pierce	$66.33
DSS	Disuccinimidyl suberate	1 g	Pierce	$106.00
Other				
Gal	4-aminophenyl beta-d-galactopyranoside	100 mg	Sigma	$52.40
Total				$417.18

2.4 Statistical Basis of Experiments

In all testing, samples are made in at least triplicate, in separate tubes. The statistical significance was evaluated by conducting unpaired, one-tailed t-tests assuming unequal variance between two groups. The statistics were calculated using Excel. One-tailed tests were conducted because data is typically analyzed for an increase or decrease in signal and unequal variance is used because little is known about the materials being tested and unequal variance is more conservative.

CHAPTER 3: METHODS

3.1 Aim 1: Synthesis and Purification

3.1.1 Synthesis Strategy 1a: Solid Phase Peptide Synthesis (product: R9-G3-TP)

FMOC solid phase peptide synthesis (SPPS) on a 0.1 mmol scale was used to synthesize the peptide sequence RRRRRRRRRGGGFQHPSFI. Four-molar excess of each Fmoc amino acid from Novabiochem and peptide Coupling Reagent HBTU (Protein Technologies, Inc) was added to each amino acid cartridge. 0.1 mmol of Fmoc-Ile-Wang resin (0.61 mmol/g, Novabiochem) was used with DMF as the Solvent, 0.4M N-Mehtylmorpholine/DMF as Activator (Protein Technologies, Inc), and 20% (v/v) piperidine/DMF as the Deprotector. The reaction was carried out under nitrogen in the PS3 (Protein Technologies, Inc).

For analysis, the peptide was cleaved from dried resin with 10 mL/gram resin of cleavage cocktail (95% TFA + 2.5% TIPS + 2.5% dH_2O). Cleaved peptide collected, then precipitated out with chilled ethyl ether and pelleted by centrifuging at 4000 rpm for 5 min at -4^{o}C. Chilled ether is decanted and peptide is re-suspended in fresh ether 3 times. The peptide is allowed to air dry for at least 3 hrs.

3.1.2 Synthesis Strategy 1b: Heterobifunctional Crosslinking (product: R9-SS-TP)

First, FMOC (SPPS) to synthesize the R9 peptide (seq: RRRRRRRRR) and the targeting peptide, denoted TP (seq: FQHPSFI). Second, the heterobifunctional crosslinkers SMPB (reactive toward amino and sulfhydryl groups) and SATP (reactive toward amino and maleimide groups) were conjugated to TP and R9, respectively. Finally, SMBP-TP was conjugated to SATP-R9 to form R9-SS-TP.

3.1.2.1 Peptide Synthesis

3.1.2.1.1 Original Peptide Synthesis Protocol

In the original protocol, FMOC SPPS on a 0.1 mmol scale was performed as described in section 3.1.1.

3.1.2.1.2 Modified Peptide Synthesis Protocol

In the modified protocol for R9, FMOC SPPS from section 3.1.1 was modified to use HATU as the peptide Coupling Reagent, 50%DMF/50%DMSO as the Solvent, and 2%DBU/2%Piperidine as the Deprotector.

In the modified protocol for TP, FMOC SPPS from section 3.1.1 was modified to use 50%DMF/50%DMSO as the Solvent and 2%DBU/2%Piperidine as the Deprotector.

3.1.2.2 SMPB-TP

40-fold molar excess of TEA was added to 0.05 mmol dried TP resin dissolved in 5mL DMSO and stirred at RT for 17 min to deprotonate primary amines. 2.17-fold molar excess SMPB was dissolved in 4.72 mL DMSO. The SMPB solution was added to the resin and stirred at RT for 1hr. SMPB-TP resin was rinsed 5 times with DMF to remove excess SMPB.

Reaction was carried out a second time with 20-fold molar excess TEA and 2.2-fold molar excess SATP in a total of volume of 10 mL DMSO.

3.1.2.3 SATP-R9

40-fold molar excess TEA was added to 0.0 5mmol dried R9 resin dissolved in 5 mL DMSO and stirred at RT for 10 min to deprotonate primary amines. 6.67-fold molar excess SATP was dissolved in 4.72 mL DMSO. The SATP solution was added to the resin and stirred at RT for 1hr. SATP-R9 resin was rinsed 5 times with DMF to remove excess SATP.

Reaction was carried out a second time with 20-fold molar excess TEA and 2.2-fold molar excess SATP in a total of volume of 10 mL DMSO.

3.1.2.4 R9-SS-TP

10 mL of 0.5 M hydroxylamine and 25 mM EDTA disodium salt in PBS, pH 7.4 was prepared. The solution was added to 0.05 mmol dried SATP-R9 resin and stirred at RT for 2 hrs. 0.05 mmol dry SMPB-TP (cleaved from resin) was added to solution and stirred at RT for 3 hrs.

In a second round of reactions, 0.5 M hydroxylamine and 25 mM EDTA disodium salt was prepared in 5 mL dH_2O + 5 mL DMSO. The solution was added to 0.05 mmol dried resin from the first reaction and stirred at RT for 6 hrs. SMPB-TP leftover from the previous reaction was dissolved in 10 mL DMSO was added to resin solution. The reaction was stirred at RT for 40 hrs.

3.1.3 Synthesis Strategy 1c: Homobifunctional Crosslinking (product: R9-DSS-TP)

20-fold molar excess TEA was added to 0.03 mmol R9 resin in 916.4 µL DMF for a total volume of 1 mL to deprotonate amines. The reaction was stirred at RT for 15 min. 10-fold molar excess DSS was added to R9 solution and stirred at RT for 1 hr. The R9 resin was rinsed 5 times with DMF to remove excess DSS. 5-fold molar excess NHS was added to R9 resin in 976.76 µL DMF. 5-fold molar excess DIC was then added to R9-DSS solution and allowed stir at RT for 30 min to regenerate maleimide groups. 15 min before NHS/DIC reaction completed, TEA at 20-fold excess to TP, was added to 0.03 mmol TP (cleaved from resin) in 916.4 µL DMF for a total volume of 1 mL to deprotonate amines. The TP reaction is stirred at RT for 15 min. The R9 resin was rinsed 5 times with DMF to remove excess DIC/NHS. Washed resin was added to TP solution and stirred at RT for 2 hrs. Resin was rinsed with DMF to remove excess reactants.

3.1.4 Synthesis Strategy 2b: Synthesis with Galactopyranoside (product: R9-DSS-Gal)

20-fold molar excess TEA was added to 0.03 mmol R9 resin in 916.4 µL DMF for a total volume of 1 mL. The reaction was stirred at RT for 15 min. 10-fold molar excess DSS was added to R9 solution and stirred at RT for 1 hr. The R9 resin was rinsed 5 times with DMF to remove excess DSS. NHS at 5-fold molar excess to R9 was added to R9 resin in 976.76 µL DMF (for total reaction volume of 1mL). DIC at 5-fold molar excess to R9 was then added to R9-DSS solution and allowed stir at RT for 30 min. 15 min before DIC reaction completed, TEA at 20-fold excess to Gal (4-aminophenyl beta-d-galactopyranoside) was added to 0.15 mmol Gal in 582 µL DMF for a total volume of 1 mL. The Gal reaction is stirred at RT for 15 min. The R9 resin was rinsed 5 times with DMF to remove excess DIC/NHS. Washed resin was added to Gal solution and stirred at RT for 2 hrs. Resin was rinsed with DMF to remove excess reactants.

3.1.5 Analysis by Mass Spectrometry

The dried peptide was dissolved at in 49.5% methanol + 49.5% dH_2O + 1% glacial acetic acid for analysis on an Esquire electrospray ion trap mass spectrometer from Bruker Daltonics, unless otherwise stated.

3.1.6 Analysis and Purification by High Performance Liquid Chromatography

Analysis was carried out by injecting 20 µL of sample into a C12 analytical scale column (Jupiter 4u Proteo 4.6x250, Phenomenex) and adjusting a gradient between water and ACN.

Purification of the raw R9-DSS-TP product was carried out by injecting 500 µL of sample at a time into a C12 semi-prep scale HPLC column (Jupiter 4u Proteo 10x250 mm 4 micron, Phenomenex). The sample was fractionated into 5 peaks after optimizing the water/ACN gradient and each of the fractions was collected manually. Mass spectrometry was used to analyze a sample of each peak.

3.2 Aim 2: Characterization

3.2.1 DNA Condensation

DNA was labeled with a fluorescent dye that is quenched upon electrostatic complexation with a polymer. Fluorescence signal was measured to determine concentration of polymer at which DNA is condensed.

A solution of 0.1 mg/ml DNA (gWiz Luciferase) with 1 mol YOYO1 dye for each 25 mol DNA base pair was prepared in HBG (20 mM HEPES, 5% glucose w/v). DNA-YOYO1 was incubated at 50^{o}C for 2 hours to allow dye to equilibrate among DNA strands. Polyplexes were made by adding 31uL polymer to 31 µL DNA-YOYO1 (for triplicate) and allowing polyplexes to form for 20 min at RT. 20 µL of each polyplex solution was added to each well of a black, clear-bottom 96-well plate (or 10 µL of DNA-YOYO1 solution for N/P 0). 80 µL HBG was added to each well (or 90uL HBG for N/P 0) for final volume of 100 µL. Fluorescence was measured with excitation wavelength of 491 nm and emission wavelength of 513 nm (with bandwidths set to 5nm) on an XFLuro4SafireII plate reader (Tecan).

3.2.2 Particle Sizing and Zeta Potential

The polyplex size (in terms of hydrodynamic diameter), and surface charge (in terms of the zeta potential), were measured by dynamic light scattering for various N/P ratios.

25 µL of polymer was added to 25 µL of 0.1 mg/ml DNA (gWiz Luciferase) and allowed to form polyplexes for 20 min at RT. Sizing samples were diluted in 550 µL HBG (20 mM HEPES, 5% glucose w/v) and zeta potential samples were diluted in 1100 µL HBG and 550 µL dH_2O before measurement on a ZetaPALS Zeta Potential Analyzer (Brookhaven Instruments Corporation).

3.2.3 Cellular Toxicity

Cellular toxicity was measured by providing cells (previously incubated with polymers of interest) with a substrate, MTS, that is cleaved by a mitochondrial enzyme. The substrate and

product have different absorption spectra, which can be correlated to the amount of cellular activity

HepG2 cells were plated at 100 µl/well of $1x10^5$ cells/ml in complete media (ATCC-formulated Eagle's Minimum Essential Medium with 10% fetal bovine serum and 1% antibiotics) on a 96-well plate. After incubating for 24 hours, 200 µl of free polymer was added to each well. Two-fold serial dilutions, starting with N/P 15 concentration of each polymer, were made in triplicate. Cells were incubated for 5 hrs before polymer solutions were replaced by 100 µl complete media and incubated for 19 hrs. 20 µL MTS substrate (CellTiter 96® AQueous One Solution Reagent) was added to each well and cells were incubated with MTS for 2 hours before reading absorbance at 490 nm on an XFLuro4SafireII plate reader (Tecan).

3.3 Aim 3: Evaluation

3.3.1 Transfection Ability

Cells are incubated with polyplexes formulated with the reporter gene Luciferase. Cells that are successfully transfected will express the Luciferase enzyme. Addition of Luciferase substrate results in chemiluminescence, which was normalized by total protein content of each sample to account for differences in cell plating. Protein content assay is based on reduction of copper by protein in alkaline conditions.

HepG2 cells were plated at 1ml/well of $5x10^4$ cells/ml in complete MEM (ATCC-formulated Eagle's Minimum Essential Medium with 10% fetal bovine serum and 1% antibiotics) in a 24-well plate. Cells are incubated for 24 hours at 37°C. Polyplexes are made by adding 10 µl polymer to 10 µl of 0.1mg/ml DNA (gWiz Luciferase) and allowed to form at room temperature for 20 min, for 1 µg DNA per well. 180 µL Opti-MEM was added to each polyplex tube and 200 µL of polyplex solution was added to each well. Plates were incubated for 4 hrs. The polyplex solution was aspirated and cells were washed twice with PBS. 0.5 mL complete media was then added to each well and cells were incubated for 44 hrs. Media was aspirated from wells and cells were washed twice with PBS. 200 µL of 1X CCLR (Cell Culture Lysis Reagent, Promega) was added to each well. Plates were incubated at RT for 15 min then wrapped in Saran wrap and frozen at -80°C for 3 hrs to completely lyse cells. Cell lysate was collected form plates and centrifuged at 14,000 x g for 10 min at 4°C. 100 µl of supernatant was collected.

3.3.1.1 Luciferase Assay

20 µL cell lysate was added to each well of a white 96-well plate. 100 µL of luciferase substrate (Luciferase Assay System (Promega) was added to each well immediately before the luminescence was read on a plate reader. The luminescence was integrated for 1000 ms on an XFLuro4SafireII plate reader (Tecan).

3.3.1.2 BCA Total Protein Assay

BSA standards and working reagent were prepared according to manufacturer directions (Micro BCA™ Protein Assay Kit, Pierce). Lysates were diluted 1:25 in dH_2O. 100 µL of each standard of dilute sample was added to each well of a clear 96-well plate. 100 µL of working reagent was added to each well and mixed thoroughly. The plate was wrapped in Saran wrap and aluminum foil and incubated for 2 hrs. The absorbance at 562 nm was read on a plate reader.

3.3.2 Binding and Uptake

Cells are incubated with polyplexes formed with a fluorescently labeled DNA. The fluorescence signal of individual cells was read by flow cytometry to determine the amount of binding (when incubated at 4°C) or binding and uptake (when incubated at 37°C).

HepG2 or HeLa cells were plated at $11x10^4$-$30x10^4$ cells/1mL/well in 6-well plates for 15 hours at 37°C. Cells were washed with PBS once. 1 ml Opti-MEM was added to each well. Plates were then pre-incubated at 4°C or 37°C for 1 hr.

YOYO1-DNA was prepared at 0.08 µg/uL DNA (gWiz Luciferase) with 1 mol YOYO1 dye for each 25 mol DNA base pair in HBG (20 mM HEPES, 5% glucose w/v). DNA-YOYO1 was incubated at 50°C for 2 hours to allow dye to equilibrate among DNA strands. Polyplexes were prepared by adding 325 µl polymer (or HBG) to 325 µLYOYO1-DNA (for triplicates) and allowed to form for 20 min.

100 µL polyplex solution (or HBG) was added to each well and mixed by rocking plate gently. Plates were incubated at 4°C or 37°C for 2 hr. The polyplex solution was then aspirated and cells were washed with PBS twice. Cells were trypsinized with 0.5 ml 0.05% Trypsin + 0.53 mM EDTA. 1 mL complete MEM (ATCC-formulated Eagle's Minimum Essential Medium with 10% fetal bovine serum and 1% antibiotics) was added to each well. Re-suspended cells were transferred to 1.5 mL eppendorf tubes and spun

down at 4000g for HepG2 5000g for HeLa for 5 min at 4^{o}C. Media was aspirated and cells were resuspended in 1 mL complete MEM. Samples were transferred to polycarbonate tubes and kept on ice.

Flow cytometry and data analysis were conducted by Ester Kwon.

CHAPTER 4: RESULTS AND DISCUSSION

4.1 Aim 1: Synthesis and Purification

4.1.1 Synthesis Strategy 1a: Solid Phase Peptide Synthesis (product: R9-G3-TP)

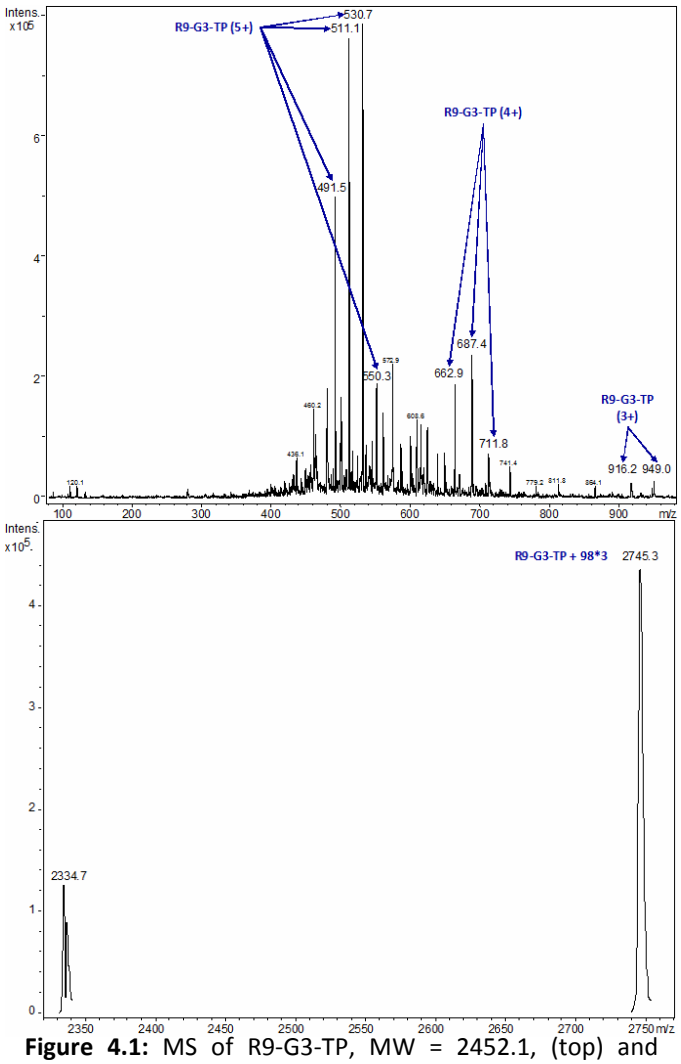

Figure 4.1: MS of R9-G3-TP, MW = 2452.1, (top) and software deconvolution (bottom). In the initial interpretation of the data, only the 491.5 m/z peak was identified to correspond to the product. In reality, most of the peaks correspond to R9-G3-TP.

After using solid-phase-peptide-synthesis (SPPS) to synthesize R9-G3-TP (seq: RRRRRRRRRGGGFQHPSFI), the product was verified by mass spectrometry (MS).

Initial analysis of the MS data on R9-G3-TP (MW = 2452.1 g/mol), shown in Figure 4.1, identified the peak at 491.5 m/z as the 5+ charge of the R9-G3-TP peptide. However, no other peaks matched that of the desired product directly. It therefore appeared the synthesis was very inefficient because most of the peaks did not correspond to product. Further, high performance liquid chromatography analysis of the peptide was inconsistent and therefore, the HPLC analysis of the peptide product was not reproducible (data not shown).

However, it was later discovered that peptides and proteins with basic residues, like arginine, form adducts of molecular mass 98 in the presence of trace sulfate and phosphate ions (Chowdhury 1990). This complicates mass spectrometry analysis of any peptide containing arginine because a single charged state is represented by multiple peaks in the spectra. Using this information, the correct interpretation of Figure 4.1 is that a majority of the peaks correspond to the 3+, 4+, or 5+ charge states of R9-G3-TP. As shown in the deconvoluted spectra, there are

contaminants, which may correspond to R9-G3-TP missing two glycines (MW = 2337.96 g/mol) or missing isoleucine (MW = 2338.93 g/mol). Due to time constraints, R9-G3-TP was neither purified nor tested.

4.1.2 Synthesis Strategy 1b: Heterobifunctional Crosslinking (product: R9-SS-TP)

Since initial results indicated that SPPS was ineffective for synthesizing R9-G3-TP, a new strategy was developed to link DNA condensing peptide R9 and hepatocarcinoma targeting peptide TP. Briefly, the peptides are synthesized separately, then crosslinking compounds were conjugated to the N-terminus of each peptide, and finally the peptides are conjugated together through their respective crosslinkers.

4.1.2.1 Peptide Synthesis

4.1.2.1.1 Original Peptide Synthesis Protocol

The MS data for the SPPS of R9 (MW = 1423.8 g/mol) using HBTU as the Coupling Reagent, DMF as the Solvent, and 20% (v/v) piperidine/DMF as the Deprotector is shown in Figure 4.2. Although many of the peaks correspond to the desired peptide R9, there was also significant signal from R8 (MW = 1267.6 g/mol), R7 (MW = 1111.4 g/mol), and R6 (MW = 955.2 g/mol). These peaks were identified by taking into account the possible total masses of the compounds,

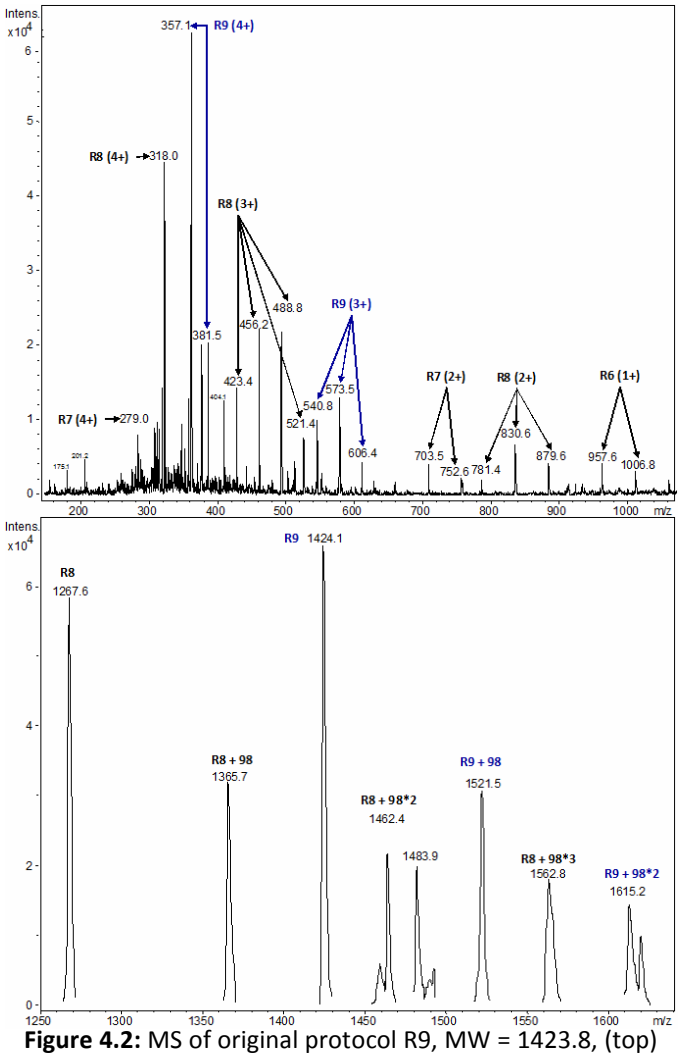

Figure 4.2: MS of original protocol R9, MW = 1423.8, (top) and software deconvolution (bottom). The resulting product contains peaks that correspond to R9, R8, R7, and R6.

possible charge states (up to the number of arginines in the compound), and possible presence of 98 g/mol adducts (Chowdhury 1990).

Because the product had significant amounts of contamination, a more efficient peptide synthesis strategy was designed.

4.1.2.1.2 Modified Peptide Synthesis Protocol

The MS data for R9 (MW = 1423.8 g/mol) synthesized using HATU as the Coupling Reagent, 50%DMF/50%DMSO as the Solvent, and 2%DBU/2%Piperidine as the Deprotector is shown in Figure 4.3. The majority of the peaks correspond R9, taking into account the possible presence of the 98 g/mol adducts (Chowdhury 1990).

Subsequent steps used the raw material from this synthesis. The R9 was not purified in order to conserve material and time.

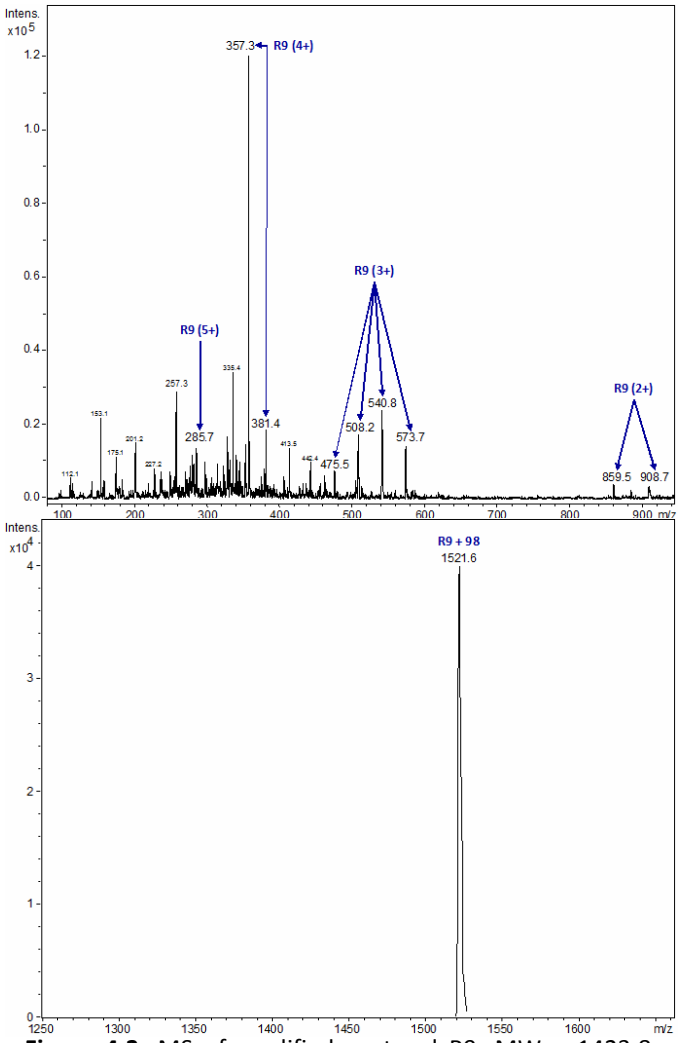

Figure 4.3: MS of modified protocol R9, MW = 1423.8, (top) and software deconvolution (bottom), dissolved in H_2O. The majority of the peaks correspond to charge states of R9, indicating the synthesis was successful.

The MS data for TP (seq: FQHPSFI, MW = 875.1 g/mol), synthesized by a modified SPPS protocol using 50%DMF/50%DMSO as the Solvent, and 2%DBU/2%Piperidine as the Deprotector that is shown in Figure 4.4. The main peaks correspond to the 1+ and 2+ charges of TP. There are some small, unidentified peaks that do not correspond to any of the simple nested subsets of the sequence of TP.

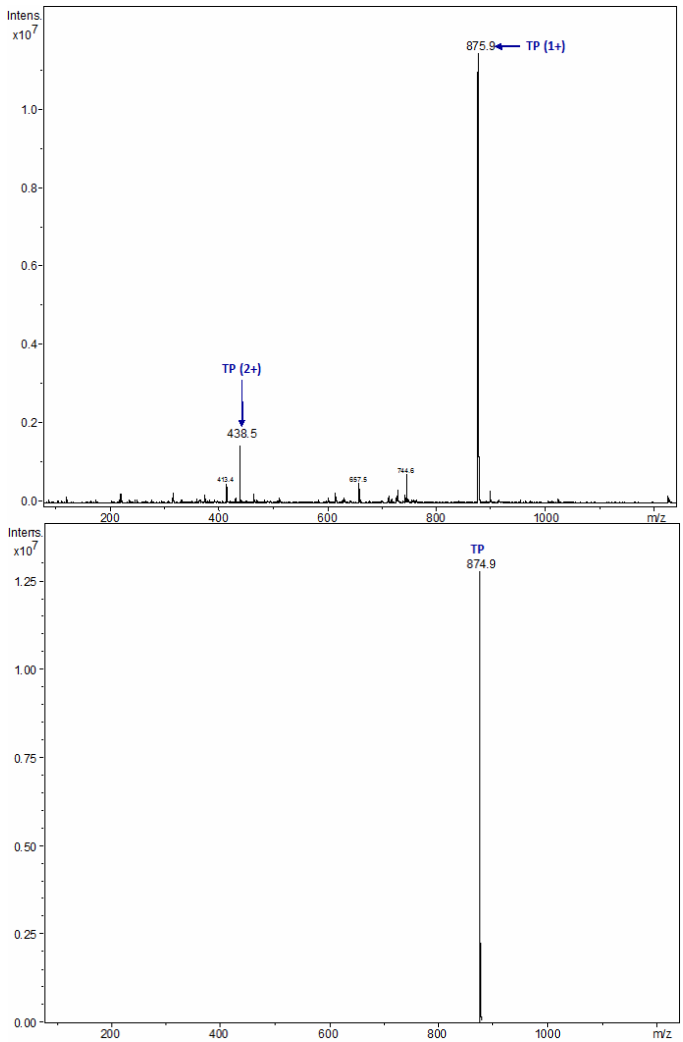

Figure 4.4: MS of TP, MW = 875.1, using the modified peptide synthesis protocol (top) and software deconvolution (bottom). The main peaks correspond to TP, but there is a small amount of unidentified contaminantion.

4.1.2.2 SMPB-TP

The crosslinker SMPB (reactive toward amino and sulfhydryl groups) was attached to the N-terminus of TP. Results from high performance liquid chromatography (HPLC) analysis of the SMPB-TP conjugation is shown in Figure 4.5. The SMPB-TP trace overlaps with the TP trace between 25 min and 30 min, indicating the presence of un-reacted TP. However, there is also a set of peaks in the SMPB-TP

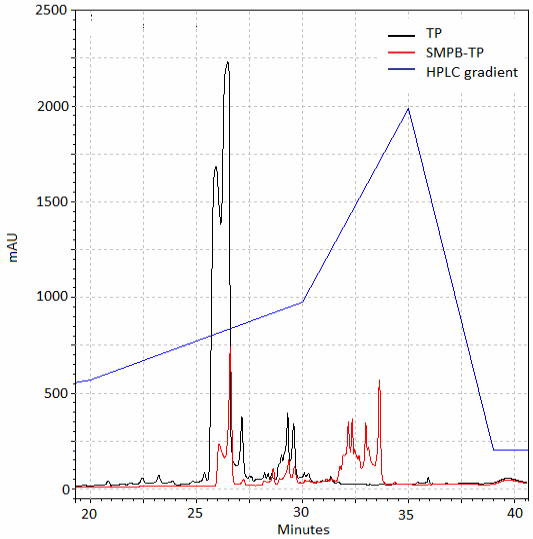

Figure 4.5: HPLC trace comparing TP (black) and SMPB-TP (red) run on the same ACN/H_2O gradient (blue). The SMPB-TP trace shows that the sample contains a new product (peaks between 30 min and 35 min), but also significant amounts of un-reacted TP (peaks between 25 min and 30 min).

sample that do not appear in the TP sample between 30 min and 35 min. This indicates that the reaction proceeded, if not to completion. From the relative sizes of the product and reactant peaks, approximately half of the TP was modified.

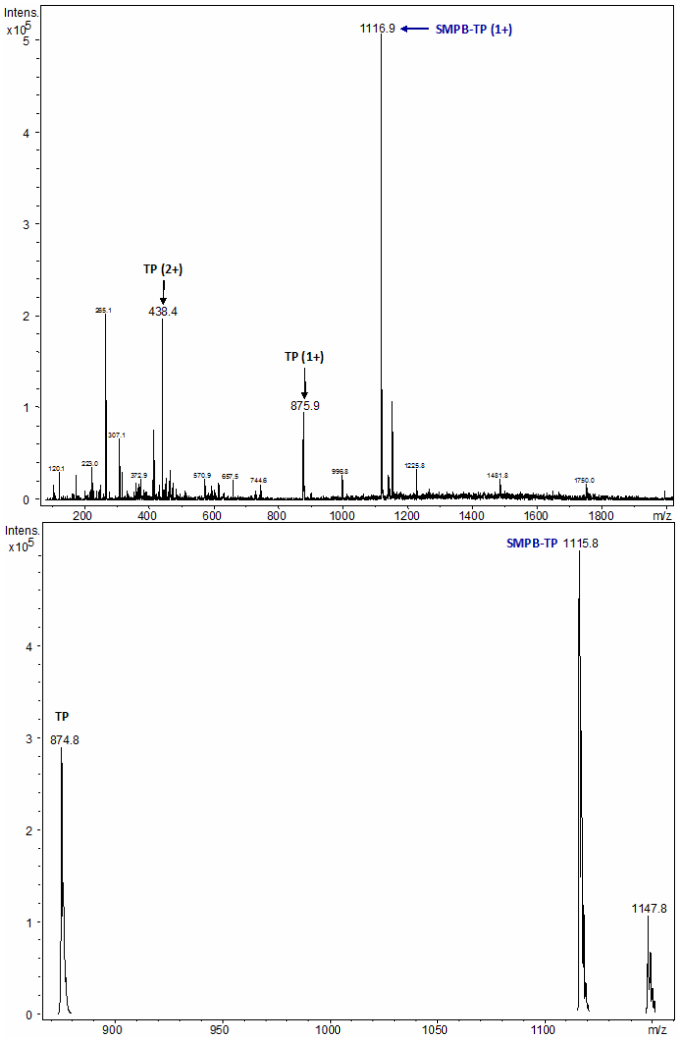

Figure 4.6: MS of SMPB-TP, MW = 1116.34, (top) and software deconvolution (bottom). There are prominent peaks that correspond to SMPB-TP, un-reacted TP, and unknown contaminants.

Mass spectrometry was conducted to verify that the HPLC product peak was indeed SMPB-TP (MW = 1116.34 g/mol). The results are shown in Figure 4.6. There is a clear 1+ charge state peak for the SMPB-TP, but also 1+ and 2+ peaks that correspond to TP. This indicated that the reaction did not go to completion.

There are also contamination peaks that are most likely due to side reactions between the SMPB, TP, TEA, and trace elements in the reaction mix. In the deconvouted MS (bottom image of Figure 4.6), the peak at 1147.8 g/mol has a difference in mass of 32 g/mol from the product peak at 1115.8 g/mol. According to the ABRF Delta Mass database, this may correspond to 3,4-dihydroxylation of proline or oxidation of proline to glutamic acid and is therefore still the desired product.

Overall, both HPLC and MS results indicated that the conjugation was effective, but inefficient. Thus, the reaction was carried out again. The MS data after the second round of reaction (not shown), was similar to Figure 4.6 an un-reacted TP remained even after the second round of reactions.

4.1.2.3 SATP-R9

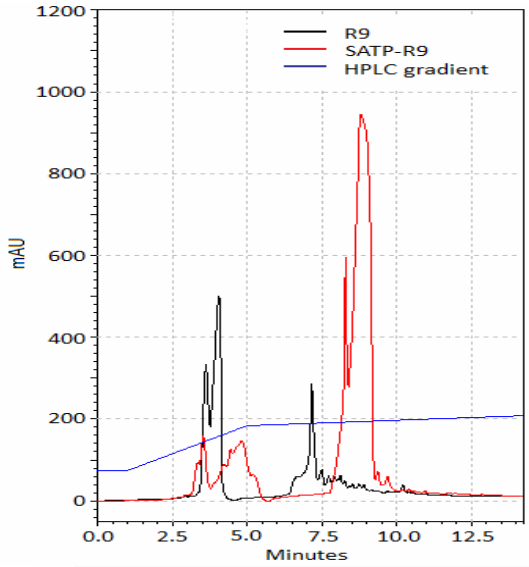

Figure 4.7: HPLC trace comparing R9 (black) and SATP-R9 (red) run on the same ACN/H_2O gradient (blue). The SATP-TP trace shows a new product (peaks between 8 min and 10 min), but also noticeable amounts of un-reacted R9 (peaks between 2.5 min and 6 min). The peaks around 7.5 min of the R9 trace is due to sample contamination.

The crosslinker SATP (reactive toward amino and maleimide groups) was attached to the N-terminus of R9. Results from HPLC analysis of the SATP-R9 conjugation is shown in Figure 4.7. Similar to the SMPB-TP conjugation results, the SATP-R9 trace indicates that a new product was made, but that not all of the R9 was modified. Judging from the relative sizes of the product peaks (8-10 min) and reactant peaks (2.5-6 min), about four-fifth of the R9 was modified. The SATP-R9 reaction was more efficient than the SMPB-TP reaction shown in Figure 4.5.

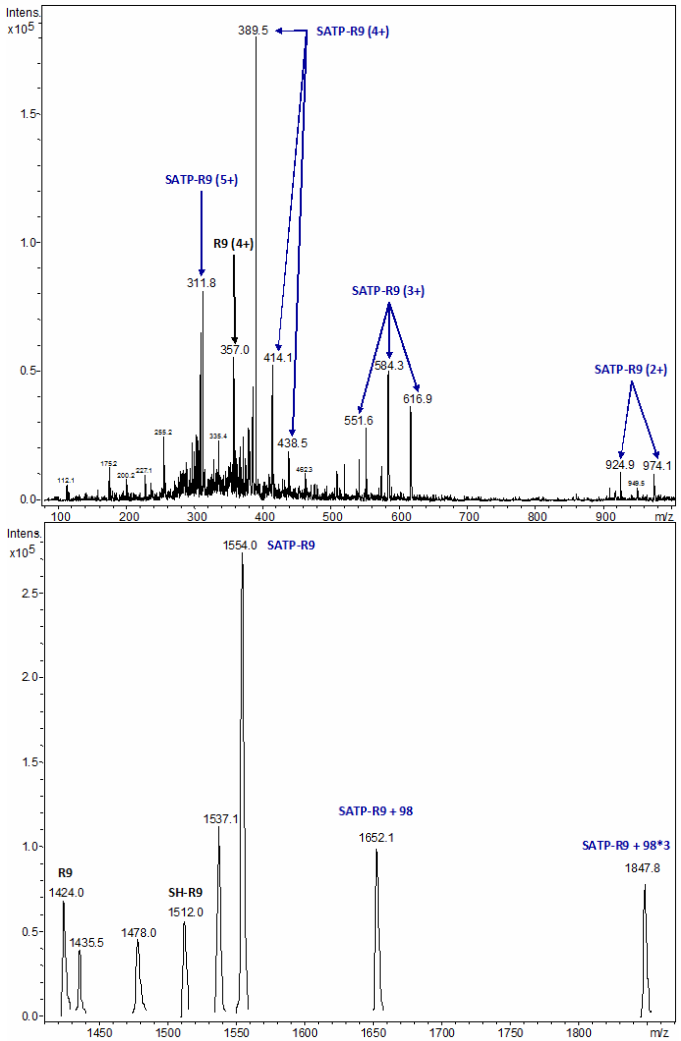

Figure 4.8: MS of SATP-R9, MW = 1554.95 (top) and software deconvolution (bottom), dissolved in H_2O. Most of the peaks correspond to SATP-R9. Also present are R9 and R9 conjugated with SATP where the sulfhydryl has been revealed (SH-R9).

Mass spectrometry results, shown in Figure 4.8, confirmed that the product SATP-R9 (MW = 1554.95 g/mol) was present. There

are also peaks that correspond to un-reacted R9 as well as to R9 that has been conjugated with SATP and has the sulfhydrl group on the SATP revealed (SH-R9, MW = 1511.95 g/mol). In general, the sulfhydrl group on SATP should be protected and is deprotected before use by addition of hydroxylamine.

There are several unknown peaks as well, which are most likely due to side reactions. For example, the peak at 1537 g/mol in the deconvoluted spectrum is probably due to the loss of water from SATP-R9 from the MS analysis process.

Overall, both the results from the HPLC and MS indicate that the conjugation of SATP-R9 was effective, but inefficient. A second round of reaction was performed and the resulting product was similar to Figure 4.8 (data not shown).

4.1.2.4 R9-SS-TP

The final step of the heterobifunctional synthesis strategy was to conjugate SATP-R9 to SMPB-TP through the free functional groups on the crosslinkers to form R9-SS-TP.

The HPLC analysis of the raw R9-SS-TP conjugation product is shown in Figure 4.9. The R9-SS-TP trace shows a peak between 28 min and 35 min that was not present in either TP or SMPB-TP. Although this indicates that some product was formed, the MS data shown in Figure 4.10 was ambiguous and not promising.

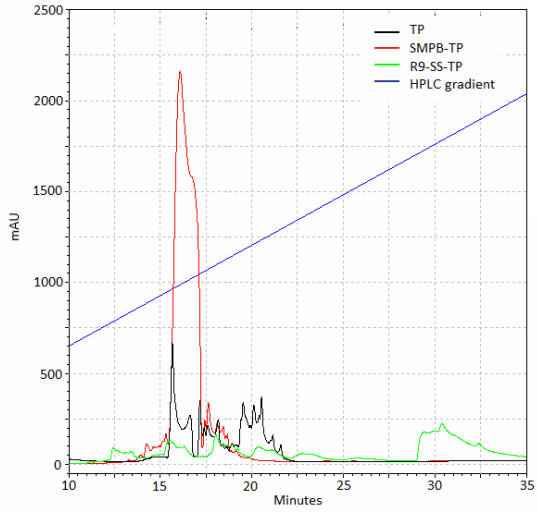

Figure 4.9: HPLC of R9-SS-TP (green) compared to TP (black), SMPB-TP (red) on the same gradient (blue). Although there is overlap with TP and SMPB-TP (15-23 min), the HPLC trace indicates that some product R9-SS-TP was formed (28-35 min).

By using the difference between sets of evenly spaced peaks in the MS, it is possible to deduce the likely charge state of the peaks. For example, the difference between 973.5 m/z, 1023.2 m/z, and 1071.9 m/z is approximately 49 m/z. This corresponds to 98/2, indicating these are the 2+ charge state. Using this type of logic, the majority of the peaks in Figure 4.10 correspond to SATP-R9. However, some of these peaks can also be correlated to R9-SS-TP. The peak at 389.4 m/z can be interpreted as the 4+ charge state of SATP-R9 or the 7+ charge state of R9-SS-TP + 98 (total MW = 2723.8 g/mol, as seen in the deconvolution), the 584.1 m/z peak can be the 5+ charge state of R9-SS-TP + 98*3

(total MW = 2919 g/mol), and the 973.5 m/z peak can be the 7+ charge state of R9-SS-TP + 98*3.

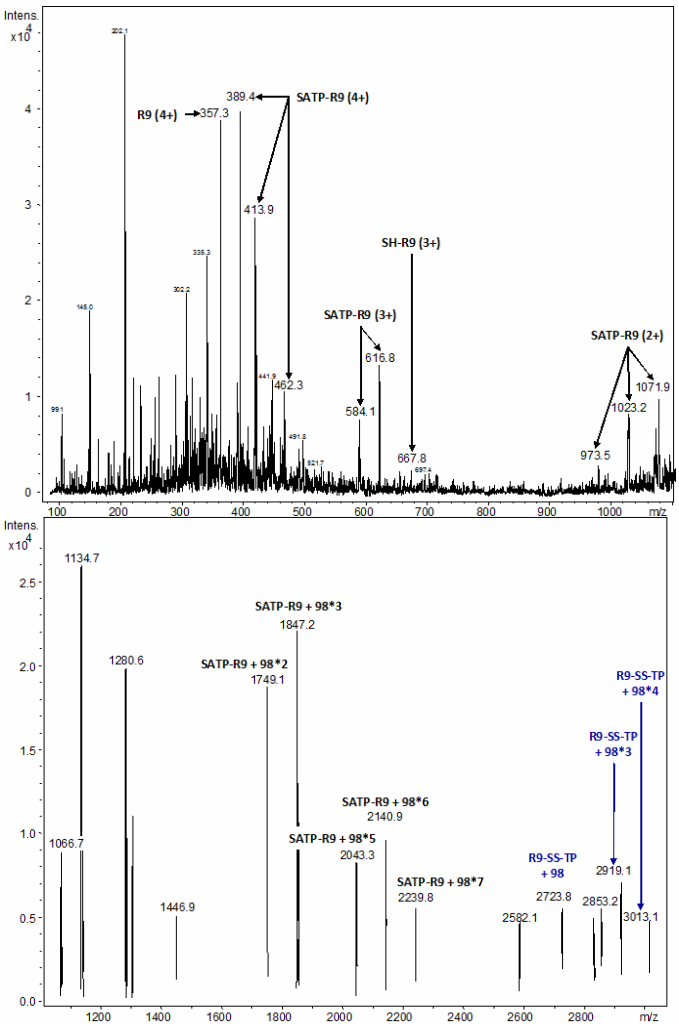

Figure 4.10: MS of R9-SS-TP, MW = 2628.29, (top) and software deconvolution (bottom). The results are ambiguous. The majority of the peaks are labeled as SATP-R9, but could be interpreted as R9-SS-TP signals.

While it would be possible to conclude that the reaction was successful, solubility issues during the conjugation indicate that the peaks should be interpreted as un-reacted SATP-R9. Specifically, hydroxylamine and EDTA were not soluble in DMSO and the peptide resin was not soluble in PBS. Therefore, although two rounds of reaction were performed and a compromise of 50%DMSO/50%H_2O was used as a solvent during the second round, little reaction occurred because components were not in solution. Also, the resin disintegrated during the second round of reactions. Therefore, even if product was recovered, this synthesis strategy introduces unnecessary contamination.

Overall, due to reactant solubility issues of the protocol and the difficulty of properly interpreting the MS results, the conjugation of SATP-R9 to SMPB-TP to was deemed unsuccessful.

4.1.3 Synthesis Strategy 1c: Homobifunctional Crosslinking (product: R9-DSS-TP)

Since MS results indicated that the heterobifunctional crosslinking protocol was ineffective at linking R9 to TP, a new strategy that emphasized simplicity and solvent

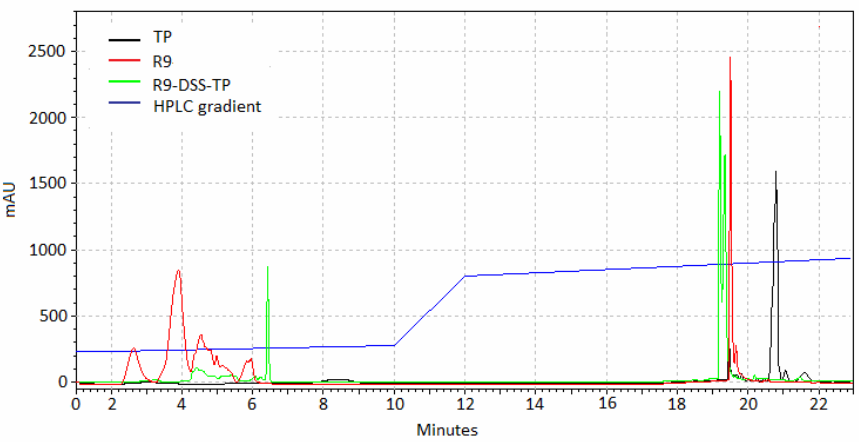

Figure 4.11: HPLC trace comparing R9-DSS-TP (green) to TP (black) and R9 (red) when run on the same ACN/H_2O gradient (blue). The R9-DSS-TP trace contains peaks that do not correspond to the peaks of either TP or R9. This indicates that a new product was formed from the reaction.

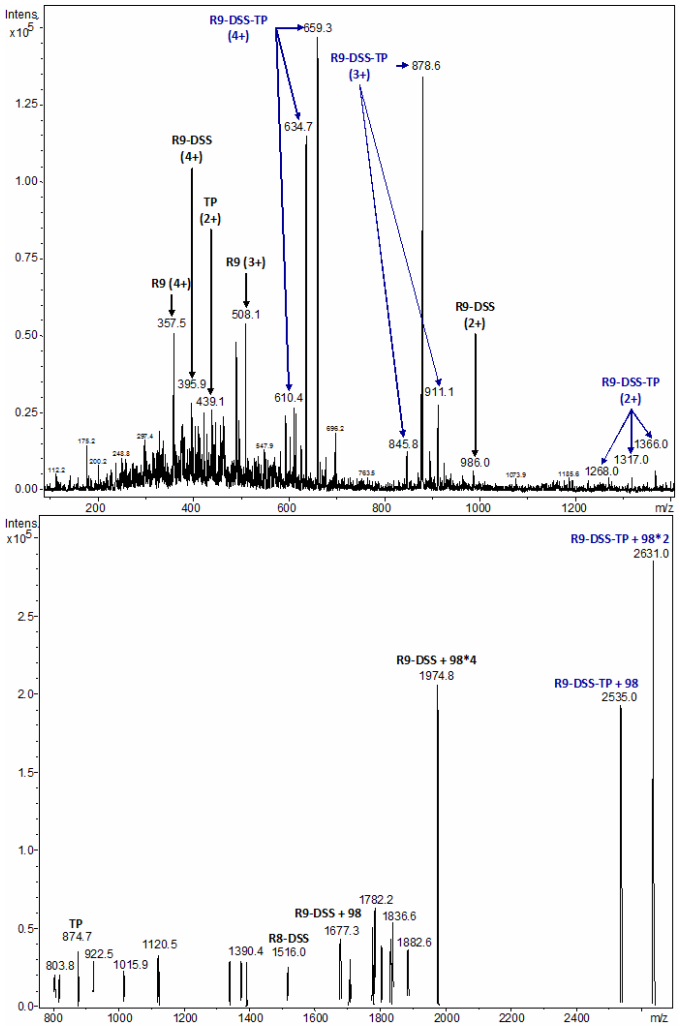

Figure 4.12: MS of R9-DSS-TP, MW = 2437.0, (top) and software deconvolution (bottom). Both spectra contain peaks that correspond to R9-DSS-TP, but also R9, TP, and incomplete crosslinking product R9-DSS.

compatibility was designed. Briefly, the peptides R9 and TP are synthesized separately and then linked together by a single, homobifunctional corsslinker, through the N-termini of each peptide to form R9-DSS-TP.

The HPLC analysis is shown in Figure 4.11. The features of the R9-DSS-TP trace at 6.5 min and 19-19.5 min are different from the reactants TP and R9. This is good indication that the reaction proceeded.

To confirm the identity of the homobifunctional rosslinking product, MS analysis was performed. The results, shown in Figure 4.12, indicate that the raw R9-DSS-TP (MW = 2437.0 g/mol) contained the desired product as well as the unmodified R9 (MW = 1423.8 g/mol), TP (MW = 875.1 g/mol), R9-DSS (MW = 1579.0 g/mol), and other contaminants. R9-DSS indicates R9 peptide that has been modified with the DSS

crosslinker, but does not have a targeting peptide conjugated to the other end of the linker. The presence of R9, TP, and R9-DSS was expected because reaction conditions were not optimized. Peak identities were calculated by taking into account molecular weights, possible charge states, and the possible presence of 98 g/mol adducts.

The unidentified peaks in the deonconvoluted spectra are most likely due to unwanted reactions such as R8-DSS.

4.1.4 Synthesis Strategy 2b: Synthesis with Gal (product: R9-DSS-Gal)

Galactose as a control for the phage-display identified targeting peptide TP. Galactose, in the form of 4-aminophenyl β-D-galactopyranoside, was attached to R9 through DSS (R9-DSS-Gal).

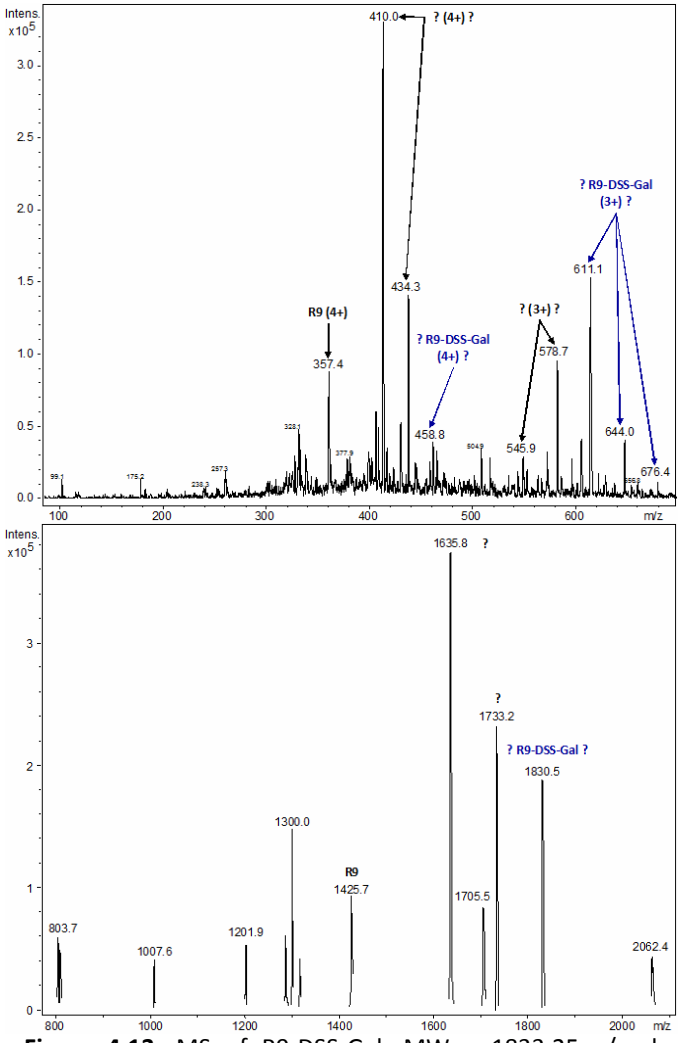

Figure 4.13: MS of R9-DSS-Gal, MW = 1833.25 g/mol g/mol, (top) and software deconvolution (bottom). The spectra was difficult to interpret because only a subset of peaks correspond to R9-DSS-Gal. Question marks indicate that labels can only be partially justified.

Figure 4.13 shows the MS results on R9-DSS-Gal (MW = 1833.25 g/mol). The spectrum is difficult to interpret because there are two sets of peaks (410.0 m/z, 434.5 m/z, 458.8 m/z and 545.9 m/z, 578.7 m/z, 611.1 m/z, 644.0 m/z, 676.4 m/z), which should correspond to the 4+ and 3+ charge states of some compound containing arginines according to the differences between the peaks (~24.5 = 98/4 and ~32.5 = 98/3, respectively). However, the lowest value in these sets of peaks (410.0 m/z and 545.9 m/z) correspond to a total mass of approximately 1635 g/mol, which does not correspond to R9-DSS-Gal or any other possible product such as R8-DSS-Gal, R7-DSS-Gal, R9-DSS, R8-DSS, or R7-DSS.

If the first two peaks in the groups are ignored, then the resulting peaks match R9-DSS-TP, as shown by the labels in Figure 4.13. Question marks on labels indicate they are only partially justified.

Since it is not clear whether the R9-DSS-Gal is present, the compound was not purified or fully characterized.

4.1.5 Purification by High Performance Liquid Chromatography

The raw R9-DSS-TP was purified by HPLC to separate R9-DSS-TP from the various other products identified in the raw MS shown in Figure 4.12. A representative trace from the HPLC during the semi-prep runs is given in Figure 4.14. Labels identify the peaks fractions collected.The MS analysis of each fraction is given in Figure 4.15.

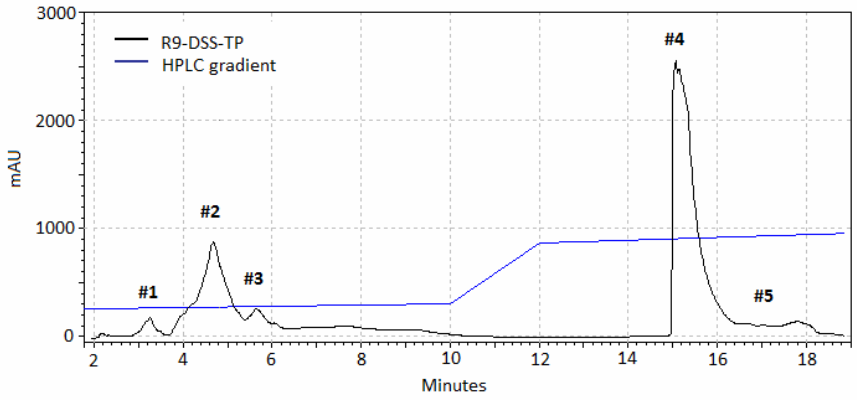

Figure 4.14: Representative HPLC trace of semi-prep purification of R9-DSS-TP. The five fractions that were collected are labeled #1-#5.

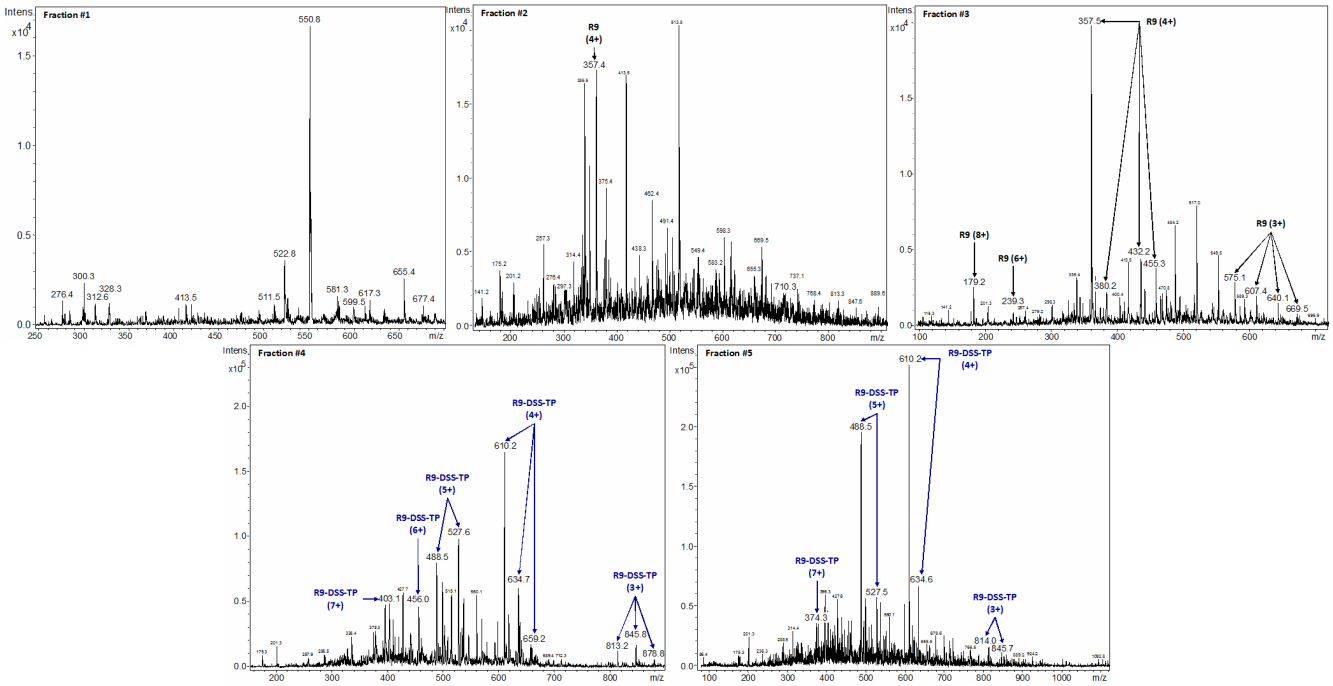

Figure 4.15: MS on semi-prep fractions of R9-DSS-TP. Fraction 1: unknown contaminants. Fraction 2: mostly contaminants, but some R9. Fraction 3: R9. Fraction 4 & 5: R9-DSS-TP.

Fraction #1 contained mostly unidentified contamination. Fraction #2 contained mostly contamination and some R9. Fraction #3 contains R9. Both fractions #4 and #5 contain R9-DSS-TP, but also some unidentified peaks. No R9 or targeting peptide signal was seen, so the major contaminants in the raw sample were successfully removed.

4.1.6 Synthesis and Purification Summary

For efficient peptide synthesis using FMOC SPPS, it was necessary to use HATU as the amino acid Coupling Reagent (for R9), 50%DMSO/50%DMF as the Solvent, and 2%DBU/2%Piperidine as the Deprotector.

The two components of this hepatocarcinoma targeting peptide based gene delivery vehicle, namely R9 for DNA packaging and TP (seq: FQHPSFI) for targeting, were successfully linked together through the homobifunctional crosslinker DSS. This identity of the product, designated R9-DSS-TP, was confirmed by MS and separated from the reaction reactants by HPLC.

The synthesis of R9 conjugated to galactose may or may not have been successful depending on the method by which MS data is interpreted. This product, designated raw R9-DSS-Gal, was neither purified nor fully characterized.

4.2 Aim 2: Characterization

4.2.1 DNA Condensation

DNA condensation, or packaging, is generally an important step in gene delivery because the process protects DNA from rapid degradation (Abdelhady 2003). Cationic polymers or peptides are capable of electrostatically condensing DNA.

Results for a YOYO1 quenching assay to measure DNA condensation ability of R9-DSS-TP and controls R9, poly-L-lysine (PLL), and polyethyleneimine (PEI) are shown in Figure 4.16. As expected, the control cationic polymers PLL and polyethyleneimine PEI were able to fully condense DNA, as indicated by

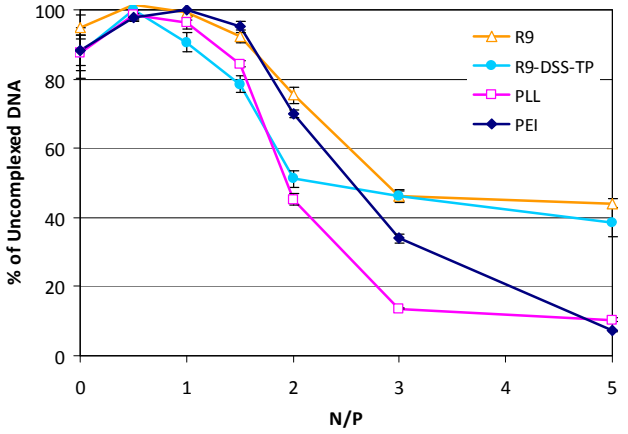

Figure 4.16: YOYO1 quenching assay to measure DNA condensation ability of polymers.

a sharp drop in fluorescence signal from the YOYO1 labeled DNA, at relatively low N/P ratios (N/P 3 and 5, respectively). Neither R9 nor R9-DSS-TP was able to condense DNA the measured N/P ratios. This is reasonable because unlike the standard polymers, these peptides do not have large numbers of charges to condense the DNA with.

However, R9-DSS-TP condenses DNA more effectively than R9, as indicated by the lower signals at almost all N/P ratios. This may be due to the hydrophobic interactions since both the linker DSS and the targeting peptide are hydrophobic.

4.2.2 Particle Sizing and Zeta Potential

The size of a polymer/DNA complex, or a polyplex, can affect its clearance, diffusion, and cellular uptake efficiency. The effective diameters, measured by dynamic light scattering (DLS), is shown in the top panel of Figure 4.17. As expected, PEI and PLL formed stable particles of size between 100-150 nm, after a certain threshold N/P ratio is reached.

Particles formed with R9 were fairly large (>150 nm) at all N/P ratios tested, indicating that the materials are aggregating or that R9 is only able to partially condense the DNA. This is consistent with the DNA condensation data, which indicates that R9 alone does not condense plasmid DNA. R9-DSS-TP particles sizes are large for small N/P, but drops dramatically at N/P 15. The targeting peptide appears to changing the way R9 interacts with DNA since R9 alone at N/P 15 does not form stable particles.

Zeta potential is a measure of the surface charge of a particle in solution. Surface charge affects delivery by influencing particle

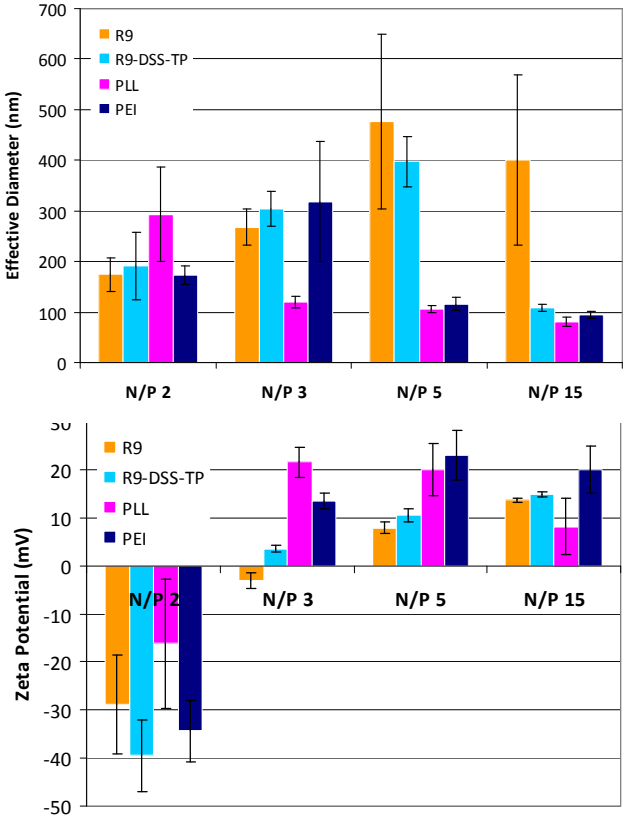

Figure 4.17: Particle sizing (top) and zeta potential (bottom) measured by dynamic light scattering. Error bars represent standard deviation over at least triplicates.

aggregation (neutral particles are more likely to aggregate than strongly charged particles) and electrostatic association. The zeta potentials, measured by DLS are shown in the bottom panel of Figure 4.17.

All materials followed the expected trend. That is, particles are negative at low N/P, become neutral. and become positive at higher N/P.

4.2.3 Cellular Toxicity

One of the drawbacks of standard cationic polymers like PEI is the relatively high toxicity of the polymer to cells (Thomas 2003). Cellular toxicity of the materials was measured by an MTS assay and presented in Figure 4.18.

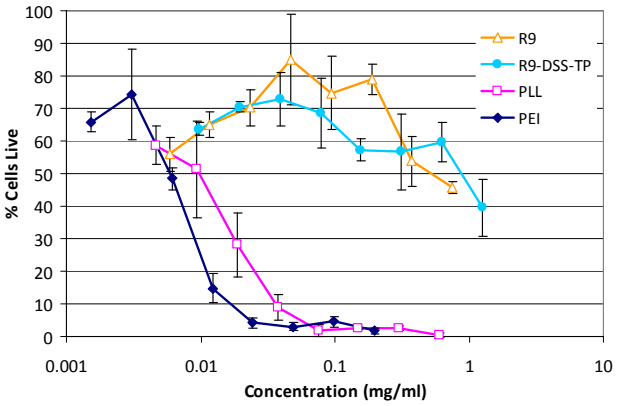

Figure 4.18: MTS assay to measure cellular toxicity of materials. Error bars represent standard deviation over triplicates.

As expected, the peptides R9 and R9-DSS-TP were significantly less toxic than either PEI or PLL in the concentration range used for transfections ($p < 0.00001$). The difference is especially pronounced at the higher concentrations.

4.2.4 Characterization Summary

The major differences between R9-DSS-TP and R9 were in DNA condensing ability and particle size. This suggests that the targeting peptide may be involved in interacting with the DNA, most likely through hydrophobic interactions between the hydrophobic residues in the targeting peptide.

4.3 Aim 3: Evaluation

4.3.1 Transfection Ability

Targeted polyplexes formed using R9-DSS-TP were expected to transfect, or delivery exogenous genes, to HepG2 cells more effectively than un-targeted polyplexes formed using R9. The transfection efficiency of the materials was evaluated by a chemoluminescence assay

based on delivering the gene for the enzyme Luciferase to cells. The amount of luminescence is normalized by the total protein content. The results are reported in Figure 4.19.

R9 and R9-DSS-TP were not significantly different in their transfection efficiency at the N/P ratios tested, but both peptides were significantly less efficient than PEI ($p < 0.01$). Compared to PLL, transfection was less efficient for the peptides the lower polymer concentrations, but at N/P 15 neither peptide was significantly different from PLL.

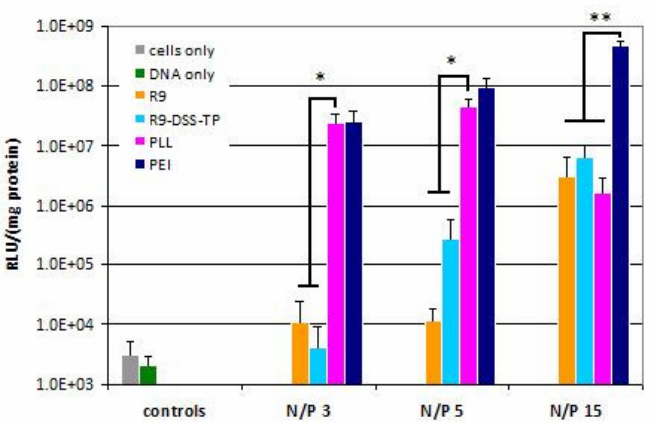

Figure 4.19: Luciferase assay normalized by BCA assay results to measure HepG2 transfection ability of materials. Error bars represent standard deviation over triplicates. * indicates $p < 0.05$ and ** indicates $p < 0.01$.

The transfection results for R9-DSS-TP and R9 tended to be more variable than for PLL or PEI, indicating that an $n > 3$ may be needed to see differences between the affect of the targeting peptide.

4.3.2 Binding and Uptake

The amount of polyplex bound to a cell surface can be determined by using flow cytometry to measure the fluorescence signal of labeled DNA. The mean fluorescence measurements of YOYO1 labeled DNA were normalized by the cells only samples and presented in Figure 4.20.

In the data shown, samples were incubated at 4°C to prevent internalization and should reflect the amount of material bound to the cell surface. Results from incubating at 37°C, which allows uptake, showed similar trends (data not shown). For both HepG2 and HeLa cells at all tested N/P ratios, the signal from R9-DSS-TP samples was significantly higher than the signal from R9 samples (p

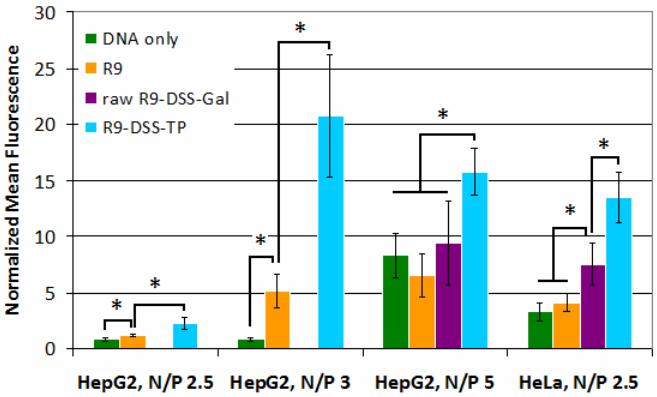

Figure 4.20: Flow cytometry mean fluorescence normalized by cell only samples to measure cell binding (cells incubated at 4°C) ability of materials. Error bars represent standard deviation over triplicates. * indicates $p < 0.05$.

< 0.05). This signifies that the targeting peptide increases the amount of DNA bound to the surface of HepG2 as well as HeLa. Since TP was reported to be nonspecific to HeLa (Zhang 2007), the increase in binding may be nonspecific rather than the desired specific targeting.

It was expected that R9-DSS-Gal would have a higher signal than R9 samples in HepG2 cells because they express ASGP receptors (Spiess 1985). However, the signal of the raw R9-DSS-Gal may be artificially lowered because the peptide was not purified and thus free galactose may compete for binding. In HeLa, the R9-DSS-Gal signal was higher than R9 ($p < 0.05$). This was unexpected because HeLa cells lack ASGP receptors (Spiess 1985).

It is difficult to draw conclusions because the fluorescence signal from YOYO1 is dependent on the degree of complexation and this property has already been shown to vary between R9 and R9-DSS-TP samples. Like the transfection data, the error bars for n = 3 were fairly high, so larger sample sizes may be necessary for proper comparisons.

4.3.3 Evaluation Summary

Despite some differences in the characteristics of polyplex formed by R9-DSS-TP and R9, this did not translate into a significant difference in the transfection of HepG2 cells. Even at N/P 15, where the R9-DSS-TP particles are significantly smaller than R9 particles, the amount of transfection was the same. Further, the peptides were much less efficient than PEI at all N/P measured and less effective than PLL at all N/P ratios except N/P 15.

Although the flow cytometry results indicated an increase in binding and uptake in HepG2 cells due to the presence of the targeting peptide, the HeLa controls suggest that the effect of TP is nonspecific.

4.4 Final Timeline

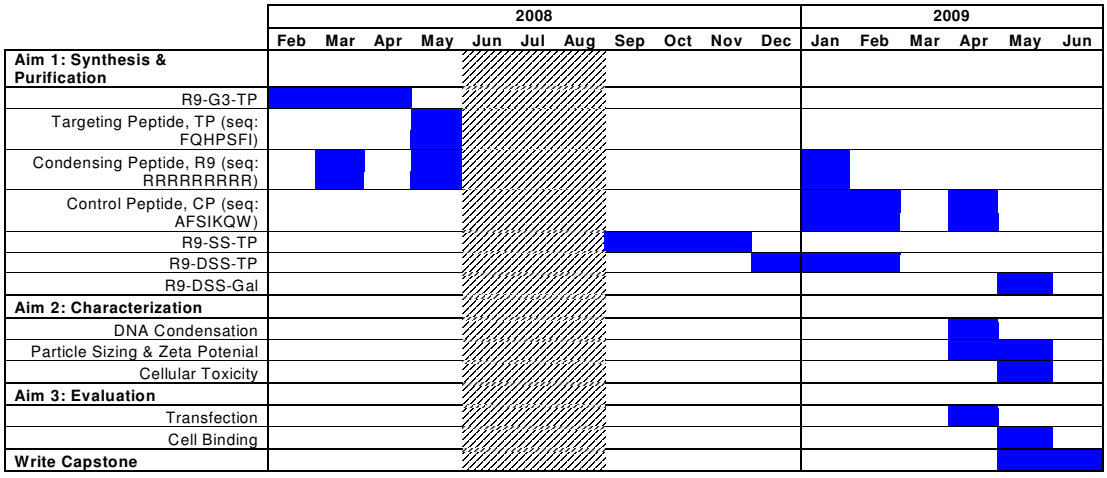

CHAPTER 5: CONCLUSIONS AND FUTURE STUDIES

5.1 Conclusions

In summary, this investigation examined the physiochemical properties and *in vitro* transfection and cellular binding ability of a gene delivery material that combined cell-penetrating peptide R9 with phage-display identified hepatocarcinoma targeting peptide TP. The tests showed that linking TP to R9 significantly changes what are generally considered important characteristics of a delivery vehicle, including increased cell binding. These differences between targeted and non-targeted R9 indicate potential for synergy between the cell-penetrating and targeting components. Such synergy would allow the effective modular design of peptide-based gene delivery materials. However, there was not the anticipated corresponding change in transfection. Clearly, our understanding of the fundamental properties that govern the effectiveness of non-viral gene delivery vehicles is still lacking and further work is needed to elucidate the governing principles that will allow truly effective rational design.

5.2 Future Studies

5.2.1 Proper Controls

R9 was not an ideal control for R9-DSS-TP because of the differences in the physiochemical characteristics of the two peptides at the same N/P. Zhang et al. identified a nonspecific 7-mer control peptide (seq: AFSIKQW) for TP. The conjugation of R9 to this control peptide via DSS would thus serve as an ideal control for R9-DSS-TP because both constructs would have the same number of amino acids and similar hydrophobicity.

5.2.2 Conjugating TP to Polymers

The small increase in transfection afforded by the specific targeting of a peptide can be easily overwhelmed by the non-specific interaction of a positively charge particle with a negative cell surface. Therefore, when testing for differences due to targeting agents, polyplexes need to be formed at an overall neutral charge (Schaffer 1998). However, neither R9 nor R9-DSS-TP was able to form stable particles at charge neutrality. Therefore, an alternative method to test the effect of targeting is to conjugate the peptide directly to a standard polymer, such as PLL or PEI. In such a formulation, DNA condensation will be afforded by the polymer and allow the formation of stable particles at neutral charge.

5.2.3 D-Amino Acids

Oligo-D-arginines have been shown to have better cell penetration as well as a tendency to label the nucleus (Wender 2000). Thus, a construct that utilizes D-arginines may prove more effective for delivering DNA. Because the constructs in this project are modular, it would easy to test different combinations of amino acid conformations for both the nonaarginine and targeting peptide components. This may elucidate interesting relations between amino acid conformation and functionality.

5.2.4 RNA Delivery

The design considerations for delivering DNA and RNA therapeutics can be quite different. For example, the two types of nucleic acids need to be packaged differently. RNA is smaller and therefore more easily complexed. RNA also needs to unpackage more efficiently than DNA in order to be effective in the cytoplasm. As the results show, R9 and R9-DSS-TP were less effective than PLL and PEI at packaging DNA and thus, may be more effective at delivering RNA.

ACKNOWLEDGEMENTS

The author was generously funded by the Mary Gates Research Scholarship and the Barry M. Goldwater Scholarship. Many thanks to Dr. Suzie Pun for the opportunity to work in her laboratory, Dr. Jamie Bergen for the conception and initial design of the project, Rob Burke for equipment training and invaluable advice throughout the project, Ester Kwon for conducting flow cytometry experiments, and the rest of the Pun lab for the gracious technical and moral support.

REFERENCES

Abdelhady HG, Allen S, Davies MC et al. *Direct real-time molecular scale visualization of the degradation of condensed DNA complexes exposed to DNase I*. Nucleic Acids Res. 2003; 31: 4001-4005.

Boussif, O, Lezoualc'h F, Zanta MA et al. *A versatile vector for gene and oligonucleotide transfer into cells in culture an in vivo: polyethyleiminie*. PNAS USA 1995; 92: 7297-7301.

Burke RS, Pun SH. *Extracellular Barriers to in Vivo PEI and PEGylated PEI Polyplex-Mediated Gene Delivery to the Liver*. Biocnjugate Chem. 2008; 19: 693-704.

Buschle M, Schmidt W, Zauner W, Mechtler K, Trska B, Kirlappos H, & Birnstiel ML. *Transloading of tumor antigen-derived peptides into antigen-presenting cells.* PNAS USA 1997; 94(7): 3256-3261.

Chowdhury SK, Katta V, Beavis RC, Chait BT. *Origin and Removal of Adducts (Molecular Mass = 98 u) Attached to Peptide and Protein Ions in Electrospray Inization Mass Spectra*. J Am Soc Mass Spectrom 1990; 1: 382-388.

Collier L, Oxford J. Human Virology. Oxford: Oxford University Press, 2000.

Derossi D, Chassaing G, Prochiantz A. *Trojan peptides: the penetratin system for intracellular delivery.* Trends Cell Biol. 1998, 8(2):84-87.

Donsante A, Miller DG, Li Y, Volger C, Brunt EM, Russell DV, Sands MS. *AAV Vector Integration Sites in Mouse Hepatocellular Carcinoma*. Science 2007; 317: 477.

Du B, Qian M, Zhou Z, Wang P, Wang L, Zhang X, Wu M, Zhang P, Mei B. *In vitro panning of a targeting peptide to hepatocarcinoma from a phage display peptide library*. BBRC 2006; 342: 956-962.

Elliott G, O'Hare P. *Intercellular Trafficking and Protein Delivery by a Herpesvirus Structural Protein.* Cell 1997; 88(2):223-233.

Felgner PL et al. *Lipofection: a highly efficient, lipid-mediated DNA-transfection procedure*. PNAS USA 1987; 84: 7413.

Gérolami R, Uch R, Bréchot C, Mannoni P, Bagnis C. *Gene therapy of hepatocarcinoma: a long way from the concept to the therapeutical impact.* Cancer Gene Therapy 2003; 10:649-660.

Gius DR, Ezhevsky SA, Becker-Hapak M, Naahara N, Wei MC, Dowdy SF. Transduced $p16^{INK4a}$ Peptides Inhibit Hypophosphorylation of the Retinoblastoma Protein and Cell Cycle Progression Prior to Activation of Cdk2 Complexes in Late G_1. Cancer Res. 1999; 59: 2577-2580.

Gonzalez H, Hwang S, Davis M. New *class of polymers for the delivery of macrmolecular therapeutics.* Bioconjug. Chem. 1999; 10: 1068-1074.

Hudson D. *Methodological implications of simultaneous solid-phase peptide synthesis. 1. Comparison of different coupling procedures*. J Organic Chem 1988; 53(3): 617-624.

Hughes V, *Therapy on trial*. Nature Medicine News Feature 2007;13:1008-1009.

Khalil A, Kogure K, Futaki S et al. *Octaarginine-modified multifunctional envelope-type nanoparticles for gene delivery.* Gene therapy 2007; 14: 682-689.

Kim DT, Mitchell DJ, Brockstedt DG, Fong L, Nolan GP, Fathman CG, Engelman EG, Rothbar JB. J. *Introduction of soluble proteins into the MHC class I pathway by conjugation to an HIV tat peptide.* Immunol. 1997; 159: 1666-1668.

Kosuge M, Takeuchi T, Nakase I, Jones AT, Futaki S. *Cellular Internalization and Distribution of Arginine-Rich Peptides as a Function of Extracellular Peptide Concentration, Serum, and Plasma Membrane Associated Proteoglycans*. Bioconjugate Chem. 2008;19:656-664.

Kumar P, Wu H, McBride JL, Jung K, Kim MH, Davidson BL, Lee SK, Shankar P, Manjunath N. *Transvascular delivery of small interfering RNA to the central nervous system*. Nature 2007;448:39-43.

Kwon EJ, Bergen JM, Park IK, Pun SH. *Peptide-mdified vectors for nucleic acid delivery to neurons.* Journal of Controlled Release 2008; 132: 230-235.

Kwon EJ, Bergen JM, Pun SH. *Application of an HIV gp41-Derived Peptide for Enhanced Intracellular Trafficking of Synthetic Gene and siRNA Delivery Vehicles*. Bioconjugate Chem. 2008; 19: 920-927.

Lin YZ, Yao S, Veach RA, Torgerson TR, Hawiger J. *Inhibition of Nuclear Translocation of Transcription Factor NF-κB by a Synthetic Peptide Containing a Cell Membrane-permeable Motif and Nuclear Localization Sequence***.** J. Biol. Chem. 1995, 270:14255-14258.

Lindgren M, Hallbrink M, Prochiantz A, Langel U. *Cell-penetrating peptides*. Trends Pharmacol. Sci. 2000; 21: 99-103.

Longmuir KJ, Robertson RT, Haynes SM, Baratta JL, Waring AJ. *Effective Targeting of Liposomes to Liver and Hepatocytes In Vivo by Incorporation of a Plasmodium Amino Acid Sequence*. Pharmaceutical Research 2006;23:759-769.

Martin ME, Rice KG. *Peptide-guided Gene Delivery.* AAPS 2007; 9(1): E18-E29.

Nagahara H, Vocero-Akbani AM, Snyder EL, Ho A, Latham DG, Lissy NA, Becker-Hapak M, Ezhevsky SA, Dowdy SF. Transduction of full-length TAT fusion proteins into mammalian cells: TAT-p27^{Kip1} induces cell migration. *Nat. Med. 1998; 4:1449-1452.*

National Cancer Institute, *Liver Cancer* [online]. Available: http://www.cancer.gov/cancertopics/types/liver/ [accessed 24 April 2008]

Otte A, Mueller-Brand J, Dellas S, Nitzsche EU, Herrmann R, Maecke HR. *Yttrium-90-labelled somatostatin-analogue for cancer treatment*. Lancet 1998; 351: 417-418.

Pack DW, Hoffman AS, Pun S, Stayton PS. *Design and development of polymers for gene delivery*. Nature Reviews 2005; 4: 581-593.

Park IK. Lasiene J, Chou SH, Horner PJ, Pun SH. *Neuron-specific delivery of nucleic acids mediated by Tet1-modified poly(ethylenimine)*. J Gene Med 2007; 9: 691-702.

Pepinsky RB, Androphy EJ, Corina K, Brown R, Barsoum J. *Specific Inhibition of a Human Papillomavirus E2 Trans-Activator by Intracellular Delivery of Its Repressor*. DNA Cell Biol. 1994; 13: 1011-1019.

Pharmalicensing.com, *China's liver cancer drug market to quadruple by 2001* [online] Available: http://pharmalicensing.com/public/press/view/1192180012_470f392c886c2/chinas-liver-cancer-drug-market-to-quadruple-by-2011 [accessed 23 April 2008]

Plank C, Tang MX, Wolfe AR, Szoka FC. *Branched cationic peptides for gene delivery: role of type and number of cationic residues in formation and in vitro activity of DNA polyplexes*. Hum. Gene Ther. 1999; 10: 319-332.

Pooga M, Hallbrink M, Zorko M, Langel U. *Cell penetration by transportan.* FASEB J. 1998; 12: 67-77.

Rudolph C, Sieverling N, Shillinger U, Lesina E, Plank C, Thünemann AF, Schönberger H, Rosenecker J. *Thyroid hormone (T3)-modification of polyethyleneglycol (PEG)-polyethyleneimine (PEI) graft copolymers for improved gene delivery to hepatocytes*. Biomaterials 2007;28:1900-1911.

Ryan KJ, Ray CG (editors) (2004). *Sherris Medical Microbiology* (4th ed. ed.). McGraw Hill. pp. 733–8.

Sachdeva MS. *Drug targeting systems for cancer chemotherapy*, Expert Opin. Invest. Drugs 1998; 1849-1864.

Sagara K, Kim SW. *A new synthesis of galactose-poly(ethylene glycol)-polyethyleniminie for gene delivery to hepatocytes*. J Controlled Rel. 2002; 79: 271-281.

Schaffer DV, Fidelman NA, Dan N, Lauffenburger DA. *Vector unpacking as a potential barrier for receptor-mediated polyplex gene delivery*. Biotechnol. Bioeng. 2000; 67: 598-606.

Schaffer DV, Lauffenburger DA. *Optimization of cell surface binding enhances efficiency and specificity of molecular conjugate gene delivery*. J. Biol. Chem. 1998; 273: 28004-28009.

Schwarze SR, Ho A, Vocero-Akbani A, & Dowdy SF. *In vivo protein transduction: delivery of a biologically active protein into the mouse.* Science 1999; 285, 1569-1572.

Simeoni F, Morrris MC, Heitz F, & Divita G. *Insight into the mechanism of peptide-based gene delivery system MPG: implications for delivery of siRNA into mammalian cells*. Nucleic Acids Res 2003; 31(11): 2717-2724.

Smith GP. *Filamentous fusion phage: novel expression vectors that display cloned antigens on the virion surfaces.* Science 1985; 228:1315-7.

Snyder EL, Dowdy SF. *Recent advances in the use of protein transduction domains for the delivery of peptides, proteins and nucleic aids in vivo*. Expert Opin. Drug Delievery 2005; 2: 43-51.

Spiess M, Lodish HF. *Sequence of a second human asialoglycoprotein receptor: Conservation of two receptor genes during evolution.* PNAS. 1985; 82: 6465-6469.

Thomas M, Klibanov AM. *Non-viral gene therapy; polycation-mediated DNA delivery*. Appl Microbiol Biotech 2003; 62: 27-34.

Torchilin VP. *Drug targeting*, Eur. J. Pharm Sci 2000; 11 (Suppl. 2): S81-S91.

Vives E, Brodin P, Lebleu B. *A truncated HIV-1 Tat protein basic domain rapidly translocates through the plasma membrane and accumulates in the cell nucleus*. J Biol Chem 1997; 272:16010-16017.

Vocero-Akbani AM, Vander-Heyden N, Lissy NA, Ratner L, Dowdy SF. Killing HIV-infected cells by transduction with an HIV protease-activated caspase-3 protein*. Nat. Med. 1999, 5: 29-33.*

Wadhwa MS, Collar WT, Adami RC, McKenzie DL, Rice KG. *Peptide-mediated gene delivery: influence of peptide structure on gene expression.* Bioconjug Chem 1997; 8: 81-88.

Wagner E, Plank C, Zatloukal K, Cotton M, Birnstiel ML. *Influenza virus hemagglutinin HA-2 N-terminal fusogenic peptides augment gene transfer by transferring-polylysine-DNA complexes: toward a synthetic virus-like gene-trnasfer vehicle*. PNAS USA 1992; 269: 12918-12924.

Weeke-Klimp AH, Bartsch M, Morselt HWM, Van Veen-Hof I, Meijer DKF, Scherphof GL, Kamps JAAAM. *Targeting of stabilized plasmid lipid particles to hepatocytes in vivo by means of coupled lactoferrin*. J Drug Targeting 2007; 15(9): 585.-594.

Wender PA, Mitchell DJ, Pattabiraman K, Pelkey ET, Steinman L, Rothbard JB. *The design, synthesis, and evaluation of molecules that enable or enhance cellular uptake: Peptoid molecular transporters*. PNAS 2000; 97: 13003-13008.

Wipf, Peter. Handbook of Reagents for Organic Synthesis. Wiley, John & Sons, Inc, 2005.

World Health Organization, *Cancer* [online]. Available: http://www.who.int/mediacentre/factsheets/fs297/en/index.html [accessed 24 April 2008]

Zanta M, ABoussif O, Adib A, Behr J. *In Vitro Gene Delivery to Hepatocytes with Galactosylated Polyethylenimine*. Bioconjugate Chemistry 1997; 8:839-844.

Zhang B, Zhang Y, Wang J. Zhang Y, Chen J, Pan Y, Ren L, Hu Z, Zhao J, Liao M, Wang S. *Screening and Identification of a Targeting Peptide to Hepatocarcinoma from a Phage Display Peptide Library*. Mol Med 2007;13:246-254.

Zurita AJ, Arap W, Pasqualini R. *Mapping tumor vascular diversity by screening phage display libraries*. J Control Rel 2003; 91: 183-6.

Zhu L, Ye Z, Cheng K, Miller DD, Mahato RI. *Site-specific delivery of oligonucleotides to hepatocytes after systemic administration.* Bioconjugate Chem 2008; 19(1): 290-298.